PREPARATION AND CHARACTERIZATION OF Zn-Sb BASED HIGH TEMPERATURE SOLDER ALLOYS

M.Sc. ENGINEERING THESIS

BY

MD. MASUDUR RAHMAN

Student No- 1014112004

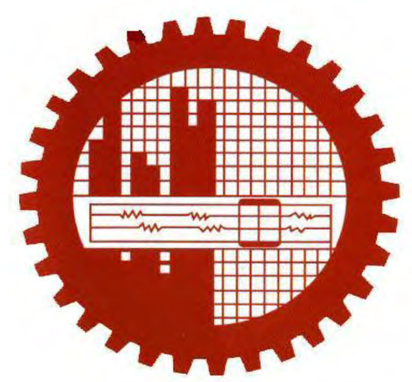

MAY 2018

DEPARTMENT OF MATERIALS AND METALLURGICAL ENGINEERING

BANGLADESH UNIVERSITY OF ENGINEERING AND TECHNOLOGY, DHAKA-1000

This thesis entitled "PREPARATION AND CHARACTERIZATION OF Zn-Sb BASED HIGH TEMPERATURE SOLDER ALLOYS", submitted by Md. Masudur Rahman, Student No. 1014112004 F, Session October 2014, has been accepted as satisfactory in partial fulfilment of the requirement for the degree of Masters of Science in Materials and Metallurgical Engineering on May 16th, 2018.

BOARD OF EXAMINERS

1.	Dr Ahmed Sharif Professor Department of Materials and Metallurgical Engineering BUET, Dhaka-1000, Bangladesh	Chairman (Supervisor)
2.	Head Department of Materials and Metallurgical Engineering BUET, Dhaka-1000, Bangladesh	Member (Ex-Officio)
3	Dr. Fahmida Gulshan Professor Department of Materials and Metallurgical Engineering BUET, Dhaka-1000.	Member
4	Dr. M. A. Gafur PSO Institute of Fuel Research & Development (IFRD) Bangladesh Council of Scientific & Industrial Research (BCSIR) Dr. Qudrat-i-Khuda Road, Dhanmondi, Dhaka-1205.	Member (External)

DECLARATION

It is hereby declared that the work presented in this thesis, except specific references are used, is result of the investigation carried out by the author under supervision of Dr. Ahmed Sharif, Professor, Department of Materials and Metallurgical Engineering (MME), Bangladesh University of Engineering and Technology (BUET).

It is also hereby declared that the work presented in this thesis has been done by the author and full or part of this thesis has not been submitted elsewhere for the award of any degree or diploma.

May, 2018

____

Md. Masudur Rahman

Student No.: 1014112004

ABSTRACT

In this study, three different compositions of the newly developed solder alloys were selected as of Zn-1.2wt% Sb, Zn-1.7wt% Sb (Eutectic alloy) and Zn-2.2wt% Sb. The pure Zinc (Zn: purity 99.99%) ingot and pure Antimony (Sb: purity 99.98%) were procured commercially and the new Zn-based Pb-free solders were developed by doping different amounts of Sb into Zn. The samples from each composition were prepared accordingly to investigate the microstructure and mechanical properties. Then ageing was carried out of the eutectic alloy at 200 °C for 250 hours and 500 hours.

X-ray Fluorescence (XRF) was done as compositional analysis. The microstructures were investigated under optical microscope (OM) and scanning electron microscope (SEM) for both as cast and aged samples. Energy Dispersive X-ray (EDX) and X-ray Diffraction (XRD) analysis were also conducted to analyze the composition and to identify the phase in the alloy respectively. The tensile strength, microhardness, electrical conductivity as well as the creep properties were observed systematically. Creep behavior was analyzed as the function of Vickers hardness at different time duration to observe the creep strain variation.

Before ageing, the eutectic Zn-1.7wt% Sb alloy exhibited the most desired characteristics among the three alloys. Later, two samples with eutectic composition were aged for 250 hours and 500 hours at same temperature 200 °C and investigated to observe the ageing effect on properties. Investigation on those three samples (as cast and aged) was narrowed down to find out Zn-1.7wt% Sb aged for 250 hours as the most appropriate high temperature solder alloy with better properties than other alloys.

Creep behavior drives the most important role in longevity and reliability of performance of any solid material. The nature of application of solder alloys demands for being in high temperature as well as high stress and both of which mostly facilitate the creep deformation in structure over the time. So, an ideal high temperature solder alloy must have well enough of creep properties to sustain and perform properly for long term. In this study, eutectic Zn-1.7wt% Sb exhibited optimum creep strain over the other two alloys. Hence, eutectic Zn-1.7wt% Sb with ageing for 250 hours was found with the required optimum properties to be the appropriate Pb-free high temperature solder alloy.

ACKNOWLEDGEMENT

The author is deeply indebted and much obliged to Dr. Ahmed Sharif, Professor, Department of Materials and Metallurgical Engineering, Bangladesh University of Engineering and Technology (BUET), Dhaka-1000 for his kind supervision and encouragement in carrying out the project work as well as in writing this thesis. His assistance through profound knowledge and experience has made the successful completion of the thesis possible.

The author is grateful to all teachers of Department of Materials and Metallurgical Engineering, BUET, Dhaka-1000 for their kind inspiration in various steps of work. The author expresses his thanks to all research students working under the supervision of Dr. Ahmed Sharif for their kind help and suggestions. Author acknowledges with appreciation the co-operation of Mr. Md. Wasim Ahmed, Mr. Md. Harunur Rashid, Mr. Ahmadullah, Mr. Md. Abdullah Al Maksud, Mr. Md. Anwar Hossain and Mr. Md. Ashiqur Rahman of Materials and Metallurgical Engineering Department.

Thanks to all the officers and staffs of the Department for their help in various stages of the study.

The author is also thankful to his employer Rahimafrooz Accumulators Limited for allowing him to pursue M.Sc. for betterment in his career.

Department of Materials and Metallurgical Engineering *The Author*

BUET, Dhaka-1000

Table of Contents

CHAPTER 1 10

INTRODUCTION 10

1.1 INTRODUCTION TO ELECTRONIC SOLDER 10

1.1.1 Definition of Solder 10

1.1.2 Soldering Mechanism 10

1.1.3 Solder alloy behavior 11

1.1.4 Intermetallic in Solders 11

1.1.5 Solderability 12

1.2 SCOPE OF STUDY 12

1.2.1 Environmental Issues and Awareness 12

1.2.2 Requirement of High Temperature Solder 13

1.2.3 Selection of High Temperature Solder 14

CHAPTER 2 15

LITERATURE REVIEW 15

2.1 ELECTRONIC INDUSTRIES AND ENVIRONMENTAL PERSPECTIVES 15

2.2 TOXIC EFFECT OF Pb...15

2.3 LEGISLATION AND DIRECTIVES 16

2.4 SOME WELL KNOWN LEAD-FREE SOLDER ALLOYS 16

2.4.1 Bi-based solder systems 16

Bi-Ag Alloys 17

Bi-Sb Alloy 18

2.4.2 Au-based solder systems 18

Au-Ge Alloy 19

Au-Sn Alloy 20

2.5 THE ELEMENT ZINC (Zn)..21

2.5.1 Zinc Based Solders 22

Zn-Mo alloy 22

Zn-Cr alloys 23

Zn-Al alloy 24

Zn-Al-Mg-Ga-Cu alloys 25

2.8 FEASIBILITY OF LEAD-FREE Zn-Sb SOLDER 28

CHAPTER 3 30

EXPERIMENTAL PROCEDURE 30

3.1 DEVELOPMENT OF NEW Pb-FREE SOLDER ALLOYS 30
3.2 THE MANUFACTURE OF Pb-FREE SOLDER ALLOYS 31
3.2.1 Raw Materials 31
3.2.2 Ingot Preparation 31
3.3 MATERIAL TEST AND CHARACTERIZATION OF Zn-xSb SOLDER ALLOY 32
CHAPTER 4 33
EXPERIMENTAL ANALYSIS, RESULTS AND DISCUSSION 33
4.1 COMPOSITIONAL ANALYSIS 33
4.1.1 X-ray Fluorescence (XRF) Analysis 33
4.2 MICROSTRUCTURAL ANALYSIS 33
*4.2.1 Microstructure under Optical Microscope (OM) and Scanning Electron Microscope (SEM)*33
4.2.2 Energy Dispersive X-ray (EDX) analysis 36
4.3 ANALYSIS ON THERMAL AND MECHANICAL PROPERTIES 38
4.3.1 Introduction 38
4.3.2 Melting Behavior Analysis 39
4.3.3 Microhardness Test 41
4.3.4 Tensile Test 42
4.3.5 Electrical Conductivity Analysis 44
4.3.6 X-ray Diffraction (XRD) Analysis 44
4.3.7 Creep Behavior Analysis 45
4.4 DISCUSSION ON OBSERVATIONS AND TEST RESULTS 47
CHAPTER 5 48
AGEING 48
5.1 INTRODUCTION 48
5.2 MICROSTRUCTURAL ANALYSIS 48
5.2.1 Microstructure under OM and SEM 48
5.2.2 Energy Dispersive X-ray (EDX) Analysis 50
5.3 ANALYSIS ON MECHANICAL PROPERTIES 51
5.3.1 Melting Behavior Analysis 51
5.3.2 Microhardness Test 53
5.3.3 Tensile Test 53
5.3.4 Electrical Conductivity Analysis 54
5.3.5 X-ray Diffraction (XRD) Analysis 55
5.3.6 Creep Behavior Analysis 55

CHAPTER 6 57
CONCLUSION....57
REFERENCES: 58
APPENDIX....62
APPENDIX A....62
(a) Zn-1.2wt% Sb: 62
(b) Zn-1.7wt% Sb(Eutectic): 62
(c) Zn-2.2wt% Sb: 62
(d) Zn-1.7wt% Sb aged for 250 hours: 63
(e) Zn-1.7wt% Sb aged for 500 hours: 63
APPENDIX B 64
APPENDIX C....65
(a) Tensile data for Zn-xSb before ageing:....65
(b) Tensile data for Zn-xSb after ageing:....65
(c) Mechanical properties for Zn-xSb before and after ageing: 65
APPENDIX D 66
(a) Creep behavior of Zn-xSb before ageing:....66
(b) Creep behavior of Zn-xSb after ageing:....66

List of Figures

Figure 2. 1 Binary Bi-Ag phase diagram [22] 17
Figure 2. 2 Microstructure of Bi-Ag solder balls: (a) Bi-2.5Ag and (b) Bi-11Ag [22] 17
Figure 2. 3 Binary Bi-Sb phase diagram....18
Figure 2. 4 Binary Au-Ge phase diagram [28] 19
Figure 2. 5 SEM image of the as-produced Au–0.28Ge eutectic alloy showing the dark (Ge) phase dispersed on the bright (Au) matrix 19
Figure 2. 6 Binary Au-Sn Phase diagram 20
Figure 2. 7 SEM images binary eutectic Au–Sn alloy showing phase transformations during thermal aging (a) as-produced, (b) 150 °C, 1 week and (c) 200°C, 1 week 21
Figure 2. 8 Binary phase diagram of Zn-Mo 22
Figure 2. 9 SEM microstructures of Zn-0.4wt%Mo & 0.6wt% Mo respectively....22
Figure 2. 10 Binary Phase diagram of Zn-Cr....23
Figure 2. 11 Microstructure of Zn-0.2wt% Cr and Zn-0.4wt% Cr respectively....23
Figure 2. 12 Binary Zn-Al phase diagram [34]....24
Figure 2. 13 Microstructure of Zn-0.3wt% Al, Zn-0.5wt% Al and Zn-0.7wt% Al respectively....24
Figure 2. 14 Binary Zn-Mg phase diagram [37]. 25

Figure 2. 15 Binary Zn-Ga phase diagram [37] 26
Figure 2. 16 Binary Zn-Sn phase diagram [40] 27
Figure 2. 17 Binary Zn-Cu phase diagram [42]. 28

Figure 3.1 Zn-Sb phase diagram 30

Figure 4.1 Optical micrographs of the chill-cast samples of Zn-1.2wt% Sb in (a) & (b) at 200X and 500X respectively, Zn-1.7wt% Sb (Eutectic) in (c) & (d) at 200X and 500X respectively, Zn-2.2wt% Sb in (e) & (f) at 200X and 500X respectively 34
Figure 4. 2 SEM microstructure in BSE mode of chill-cast samples of (a) Zn-1.2wt% Sb, (b) Zn-1.7wt% Sb (Eutectic), and (c) Zn-2.2wt% Sb (all images taken at 1000 X). 35
Figure 4. 3 SEM microstructure in SE mode of chill-cast samples of (a) Zn-1.2wt% Sb, (b) Zn-1.7wt% Sb (Eutectic), and (c) Zn-2.2wt% Sb (all images taken at 1000 X). 36
Figure 4. 4 SEM microstructure of chill-cast Zn-1.2wt% Sb with EDX spectrum at point 3 presenting 100 wt% Zn & point 4 consists eutectic composition. 36
Figure 4. 5 SEM microstructure of chill-cast eutectic Zn-1.7wt% Sb with EDX spectrum. 37
Figure 4. 6 SEM microstructure of chill-cast Zn-2.2wt% Sb with EDX spectrum. 38
Figure 4. 7 The DSC curves on heating of (a) Zn -1.2wt% Sb, (b) Zn -1.7wt% Sb (c) Zn -2.2wt% Sb [Appendix A] 40
Figure 4. 8 Microhardness values in terms of Vickers Hardness Number for different Zn-xSb solder alloys. 42
Figure 4. 9 Schematic diagram of the tensile specimen. 42
Figure 4. 10 Tensile stress-strain curves of Zn-1.2wt% Sb, Zn-1.7wt% Sb, and Zn-2.2wt% Sb solder alloys. [Appendix C] 43
Figure 4. 11 %IACS of Zn-1.2wt% Sb, Zn-1.7wt% Sb and Zn-2.2wt% Sb 44
Figure 4. 12 XRD peaks of Zn-xSb alloys. 45
Figure 4. 13 Indentation time dependence of Hardness (H) for Zn-xSb-Creep behavior 46
Figure 4. 14 Creep curves derived from Hardness (H) and Indentation time (t) for Zn-xSb [Appendix D] 46

Figure 5. 1 Optical micrographs of the chill-cast samples of Zn-1.7wt% Sb non-aged in (a) and (b) at 200X and 500X respectively, Zn-1.7wt% Sb aged for 250 hours in (c) & (d) at 200X and 500X respectively, Zn-1.7wt% Sb aged for 500 hours in (e) & (f) at 200X and 500X respectively 49
Figure 5. 2 SEM microstructure in SE mode of chill-cast samples of (a) Zn-1.7wt% Sb, (b) Zn-1.7wt% Sb aged for 250 hours, and (c) Zn-1.7wt% Sb aged for 500 hours (all images taken at 1000 X). 50
Figure 5. 3 SEM microstructure of chill-cast Zn-1.7wt% Sb aged 250 hours with EDX spectrum 50
Figure 5. 4 SEM microstructure of chill-cast Zn-1.7wt% Sb aged 500 hours with EDX spectrum 51
Figure 5. 5 The DSC curves on heating of (a) eutectic Zn -1.7wt% Sb, (b) Zn-1.7wt% Sb aged 250 hours at 200ºC, (c) Zn-1.7wt% Sb aged 500 hours at 200ºC [Appendix A] 52
Figure 5. 6 Ageing effect on microhardness of eutectic alloy 53

Figure 5. 7 Tensile strength after ageing [Appendix C] 53
Figure 5. 8 Ageing effect on electrical conductivity 54
Figure 5. 9 X-Ray diffraction patterns of non-aged and aged eutectic alloys 55
Figure 5. 10 Indentation time dependence of Hardness (H) for Zn-xSb aged for 250 hours and 500 hours-Creep behaviors 55
Figure 5. 11 Creep curves derived from Hardness (H) and Indentation time for Zn-1.7wt% Sb aged for 250 hours and 500 hours [Appendix D] 56

List of Tables

Table 3. 1 (a) Compositions of casted Zn-Sb alloys 30
Table 3. 2 (b) Ageing information 31

Table 4. 1 Compositions in XRF are given here. 33
Table 4. 2 Melting and Liquidus Temperature for different solder alloys 41
Table 4. 3 Mechanical properties of Zn-1.2wt% Sb, Zn-1.7wt% Sb and Zn-2.2wt% Sb [Appendix C] 43

Table 5. 1 Mechanical properties of Zn-1.7wt% Sb non-aged, aged for 250 hours and aged for 500 hours [Appendix C] 54

CHAPTER 1

INTRODUCTION

1.1 INTRODUCTION TO ELECTRONIC SOLDER

1.1.1 Definition of Solder

SOLDER is a fusible metal alloy exhibiting a melting point ranges from 90 to 450 °C (190 to 840 °F) and is used to be melted for joining the metallic surfaces in a process called SOLDERING. In this process, the metals must themselves have higher melting temperatures so that they remain solid when the solder is melted. It is especially useful in electronics and plumbing. Solder can contain lead and/or flux, but in many applications, solder is now lead-free. The word solder comes from the middle-English word ***soudur***, via Old French ***solduree*** and ***soulder***, from the Latin ***solidare***, meaning "***to make solid***."

1.1.2 Soldering Mechanism

Soldering is a joining process between parent materials by using a filler metal to keep parent materials solid. Soldering sometimes uses fluxing agent which is also called fluxes and it helps in cleaning the interface but may leave a residue. Because of lower processing temperatures than for brazing, soldering has been the standard assembly procedure for electronic equipment.

Usually the bond between solder and base metal is stronger than mechanical attachment, although these enhance bond strength. Rather, the essential feature of a soldered joint is that a metallurgical bond is produced at the filler-metal/base-metal interface. Heat is applied to the parts to be joined in the soldering process, causing the solder to melt and to bond to the work pieces in an alloying process called wetting. The metallurgical reactions take place between the filler metal and the base metal during solder wetting. This interaction at the solder/base metal interface can result in a covalently bonded layer of a material called an intermetallic compound. The adherence between adjacent atoms holds a piece of solid metal together which also holds the joint together upon solidification. The ease of wetting is related to the ease with which this solvent action occurs. The reaction between base-metal and filler-metal is one factor in the wetting action of the solder.

1.1.3 Solder alloy behavior

The alloy is the result of melting two or more metals together and behaves like a unique material with specific properties that can significantly differ from the properties of the individual pure metals. Alloy properties depend on the atomic structure and thermal physical properties of its constituent elements. For example, the addition of tin to lead will result in an alloy that has a lower melting point than either tin or lead—perhaps more surprisingly, so will the addition of lead to tin. The physical and mechanical properties of the alloys will also differ from the properties of the pure metals. Some combinations of metals, such as gold and silver, form alloys simply because they are mutually soluble; that is, each can be dissolved in the other. An alloy formed in such a way is called a solid solution.

Some alloy may have limited solubility in one another because of having greater differences in their basic properties and may not dissolve completely. One such combination is silver and copper, forms a eutectic alloy, which is an alloy with a melting temperature significantly lower than either of its component metals alone. The solid eutectic alloy usually exhibits a mixture comprising of two phases, rather than a solid solution and its structures and behavior are of critical importance in soldering. The melting and solidification behavior of the eutectic alloy composition itself exhibits a unique type happens at a single, specific temperature just as a pure metal does.

The covalent bond causes the intermetallic to be hard and brittle, to have a high melting point, and to be resistant to chemical attack unlike the metallic bond of metals and alloys. The physical and mechanical integrity of soldered joints can be jeopardized by excessive hard intermetallic layers.

1.1.4 Intermetallic in Solders

Intermetallic compounds act as chemical compounds than like metallic alloys. Therefore, the metal to be soldered must be metallurgically compatible with at least one of the metallic components in the solder. This intermetallic compound formation can occur by a solid/liquid reaction (molten solder against a solid base metal) or a solid-state diffusion reaction (solder plate against a solid base metal).

The intermetallic compounds form distinct phases, usually as inclusions in a ductile solid solution matrix, but they can also form the matrix itself and contain metal inclusions or form crystalline matter with different intermetallics. Those distributed finely in a ductile matrix exhibit a hard alloy; coarse structure gives a softer alloy. Intermetallics layers can thus form between the solder

and the parent material. They may cause weakening and brittleness, increase the electrical resistance of the joint or may be susceptible to electro migration and the formation of voids.

The limiting factor for base metal is to be able to form a stable intermetallic compound layer with a solder which controls the number of base-metal/solder combinations that are suitable for the majority of applications. Therefore, solderability of metals varies depending on these characteristics.

1.1.5 Solderability

Solderability is the properties of materials to ease the joining process by a given soldering method. It depends on the wettability of the two surfaces being joined. Using more active fluxes can overcome the poor component solderability to some extent, but the denser component packing makes it difficult to remove flux residue after assembly; therefore, less active fluxes are preferable. Environmental concerns are also reasons to avoid fluxes. Good component solderability is important for three basic reasons:

• It allows the use of less active fluxes, thereby reducing the requirement for cleaning flux residues.
• It produces greater first-pass soldering yields and consequently requires less hand working of the soldered joints.
• It results in a greater uniformity of solder fillet, with a geometry that is close to the ideal for maximum fatigue performance.

1.2 SCOPE OF STUDY

1.2.1 Environmental Issues and Awareness

In soldering process, Pb-based solder specially 63Sn-37Pb was mostly used previously because of its compatibility in required properties. But currently, environmental regulations around the world have targeted to eliminate the usage of Pb-bearing solders in electronic assemblies due to its inherent toxicity. Government regulations have become more adamant, and handlings of waste materials have become more regulated. This has triggered the development of Pb-free solders for the electronic industries. A successful Pb-free solder material should have the reliable properties and perform consistently over a long term. There are so many research conducted on solder material over the time like Au-based, Sn-based, Ag-based, Bi-based etc. But those have some significant drawbacks in terms of price, availability, properties, etc.

1.2.2 Requirement of High Temperature Solder

High-temperature solders have been widely used in numerous types of applications and become the prime component in electronic industries. It's not only limited in the die-attach soldering, rather extending the usage in assembling optical components, automobile circuit boards, circuit modules for step soldering, the air craft, space satellite, automotive, and oil/gas well exploration etc. [1–4]. Since the solder has to sustain in higher temperature without melting itself till the end of assembling process during soldering, so solder designing should have contained the proper melting temperature region of the solder alloy. Thus, the solidus and liquidus temperatures of high temperature solder should be designed 20 K higher and lower respectively than the maximum operating temperature [5]. In this regard, Zn-based alloys are the reasonable candidate for the high temperature solder.

High temperature solder alloys must have suitable thermal, electrical as well as mechanical properties to be reliable for longer time and to sustain in the severe thermal conditions experienced in high temperature applications such as die attachments. Thermal stress can be induced due to the incompatibility in coefficient of thermal expansion modulus; otherwise it may lead to premature failure.

The main requirements for an alternative Pb-free high temperature solder alloy are:

- **Melting point:** The melting point should be low enough to avoid thermal damage to the assembly being soldered and high enough for the solder joint to bear the operating temperatures. The solder should retain adequate mechanical properties at these temperatures. Melting temperature should be in the range of 90 °C to 450 °C
- Good **Softness** to maintain a joint structure by relaxation of thermal stress
- Good **electric and thermal conductivity** as well as appropriate **mechanical properties**
- Air tightness not to break vacuum package, **fluxless** and no alpha ray emission
- **Creep Resistance:** As the solder is supposed to perform at high temperature it is very important to ensure the creep properties of the solder.
- **Wettability:** Bonding between the solder and the metal surface is formed only when the solder wets the metal pad surface properly.
- **Availability:** There should be adequate supplies or reserves available of candidate metals. Sn, zinc (Zn), copper (Cu) and antimony (Sb) are available whereas there is a limited supply of indium (In).
- **Cost:** Manufacturers of electronic systems are unlikely to change to an alternative solder with an increased cost unless it has demonstrated better properties or there is legislative pressure to do so.

1.2.3 Selection of High Temperature Solder

There are so many research conducted during the recent years to find out a suitable Pb- free and Cd- free soldering alloy that could be used in high temperature soldering [6]. Among those high temperature Pb-free solder alloys, Au-based alloys are highly expensive, while Au–Sn alloy form brittle intermetallic compounds and thus limits the use as high temperature solder [7-8], while Bi-based alloys, especially Bi–Ag-based alloys also become brittle due to the similar reason and exhibit relatively low electrical/thermal conductivities [9-10].

Pure Zn can be used as alternative since it has excellent thermal shock resistance between -40 and 300 ˚C and low cost [11]. It is one of the best die-attachment candidates for use in next-generation wide-gap semiconductor power devices operating at temperatures up to 300°C. But, because of having brittleness due to the hexagonal close-packed (hcp) crystal structure and possess poor resistance to oxidation, a trace element addition to base metal Zn was proposed to enhance ductility and oxidation resistance of pure Zn solder for high temperature applications [12]. This addition significantly reduces the grain size of the microstructure, thus improving the tensile strength and elongation of pure Zn which enhances the interconnection ability as die-attachment candidates significantly. In contrast Zn-based alloys are more ductile comparing to others as there found no/less intermetallic compounds in these alloys, have proper melting range, good thermal/electrical conductivities [13-14], comparatively inexpensive. Numerous research works have been accomplished on Zn-based high temperature solder alloys and published in literature.

Antimony has demonstrated several advantages when used as a doping agent in solder alloys. In high temperature soldering, creep is the most important deformation mechanism and the stress-strain concentrations at the joint must be effectively relaxed by creep to ensure the solder joint reliability [15]. According to the study on creep behavior of Sn-Sb alloy, antimony has a significant strengthening effect on the solder joint by reducing the creep rate of the materials. It also improves the thermal fatigue resistance in the tin-based alloys.

In this study, antimony was selected as the added element to pure Zn because of its better creep properties, mechanical behavior, availability, low cost. The addition of fine metallic powders of Sb to Zn leads towards superior microstructural and mechanical properties which may be a suitable alternative for Pb based high temperature solder alloys.

CHAPTER 2

LITERATURE REVIEW

2.1 ELECTRONIC INDUSTRIES AND ENVIRONMENTAL PERSPECTIVES

With the advancement of technology, every industry including the electronic industries focuses on the working environment and health/safety issue (EHS) [16]. They have their own particular department to monitor the EHS to identify the aspects and impacts of environmental health risks and ensure the proper measures to eliminate that. The electronic packaging and assembly industry has the four major issues related to global environment and public health [16]:

1. Ozone-depleting Chlorofluorocarbons (CFC) elimination
2. Waste water handling
3. Volatile Organic compound (VOC) control
4. Pb content in the air and controlling of it.

Major industries have been effectively using CFCs as the most useful chemical groups for many years. They are used as a coolant in refrigeration and air-conditioning, a foaming agent for plastic-foam metals, a propellant in aerosols, and a cleaning solvent for electronics and metal industry. The threat of ozone depletion and its relation to CFCs have been recognized by both government and industry since the 1970s.

Electronic packaging and assembly plants should consider the treatment of wastewater as the major operational need not only because of the environmental effect; it also has the economic benefits. The concerns about contamination can be grouped into several areas [16]:

- pH
- Temperature
- Heavy metal
- Biological oxygen demand (BOD) and chemical oxygen demand (COD).
- Suspended solids
- Toxic chemicals or hazardous substances
- Pb content

Effluent Treatment Plant (ETP) has been used to treat and reuse of the waste water since many years. It’s a closed-loop water recycling system for a cleaning process with maintaining the pH level, segregating the toxic and hazardous substances.

2.2 TOXIC EFFECT OF Pb

Among the aforementioned concerns in electronic industries, Pb content is the most severe for the workers’ health because of its highly toxic characteristics, particularly dangerous when ingested by inhaling fumes (while melting, working with, or recycling it) or through drinking water. Toxicity of Pb has an adverse health effect on human body during accumulation for longer time.

It binds strongly to proteins in the body and inhibits normal processing and functions of the human body and facilitates Nervous and reproductive system disorder, delays in neurological and physical development, cognitive and behavioral changes, reduces production of hemoglobin resulting in anemia and hypertension [17]. The level of lead in the blood exceeds 5 mg/dl for children and 45 mg/dl for adults drives to the lead poisoning [18] and even well below level of Pb has been recognized as hazardous to a child's neurological and physical development in the recent studies.

2.3 LEGISLATION AND DIRECTIVES

The usage of Pb-bearing solders have been eliminated in the electronic industry due to environmental and health issues. As cited by the Environmental Protection Agency (EPA) of the US, Pb or Pb-bearing compound is one of the top 17 chemicals posing the greatest threat to human beings and environment [19]. Some corresponding law or directive are planned in European Union (EU), such as Waste Electrical and Electronic Equipment (WEEE), which has been come into force at December 2008 and RoHS (Restriction of certain Hazardous Substances), which is effective since 1st July 2006 [20].

In addition, many companies have publicly announced their corporate policies on development and implementation of environment friendly technologies for a variety of reasons: to sustain resources, gain market-share, avoid trade barriers, or comply with potential legislation. In the electronic industry, the Pb generated by the disposal of electronic assemblies is considered as hazardous to the environment. In Japan, the legislation prohibiting Pb from being sent to landfills and other waste disposal sites is already in place. In the US, legislations in limiting the use of Pb have been introduced in both the Senate and the House of Representatives. The legislation includes (a) H. R. 2922, The Lead Based Paint Hazard Abatement Act of 1991, (b) S. 391, the Lead Exposure Reduction Act of 1991, and (c) H. R. 3554, the Lead Exposure Act of 1992 [21].

Therefore, Pb-based solder alloys have already been considered as the most dangerous and vulnerable component for the human body due to its toxicity affected the environment and health and both Government and industries have regulated to prohibit its usage permanently.

2.4 SOME WELL KNOWN LEAD-FREE SOLDER ALLOYS

2.4.1 Bi-based solder systems

In contrast to Pb bearing solder alloys, Bismuth (Bi) is the least toxic in the group of heavy metals and it would certainly be an environment friendly Pb free solder in line with the recent increasing concerns on hazardous affect. However, pure Bi exhibits poor thermal conductivity, limited

plasticity, brittle, low tensile strength and wetting issues on common metalized surface such as Cu and Ni. Alloying elements such as Ag, Sb, Sn and so on are added to Bi as an attempt to overcome such shortcomings by creating innovative alloy microstructures and optimum alloy composition [22]. The different categories of Bi-based interconnect materials available in the literature are discussed in this section.

Bi-Ag Alloys

Bi-Ag eutectic alloy Bi-2.5wt% Ag as shown in Fig. 2.1 exhibits an acceptable melting point (262.5 °C). There is no intermetallic phase and the low solubility of silver in bismuth prohibits solid-solution strengthening. The presence of Ag rich phase in the microstructure should then result in bismuth-silver alloys being mechanically stronger and more ductile than bismuth [23]. Thus, it has a decent potential to be used as die attach solders for power devices [24].

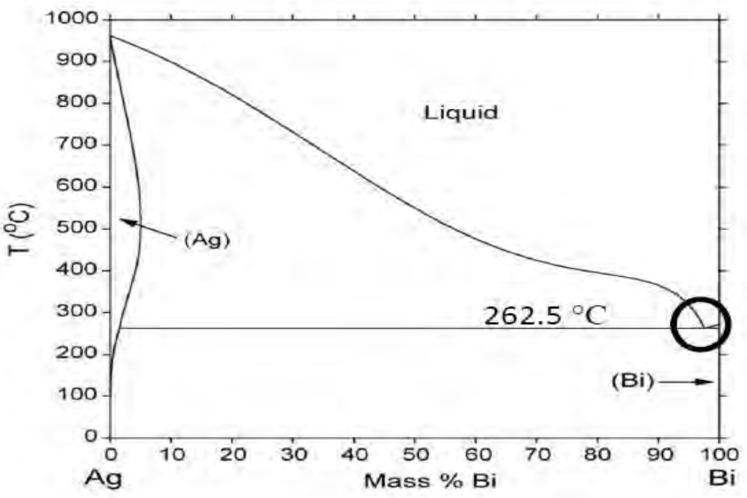

Figure 2. 1 Binary Bi-Ag phase diagram [22]

However the electrical conductivity of Bi-Ag solder is lower than that of Pb based alloy. In general, the alloys with dendritic solidification over a broad range of temperature are prone to exhibit a disparity in contraction behavior of the solid and liquid phases. This deviation can lead to several features in solder joints such as surface roughness, shrinkage voids, fillet lifting, and hot tearing.

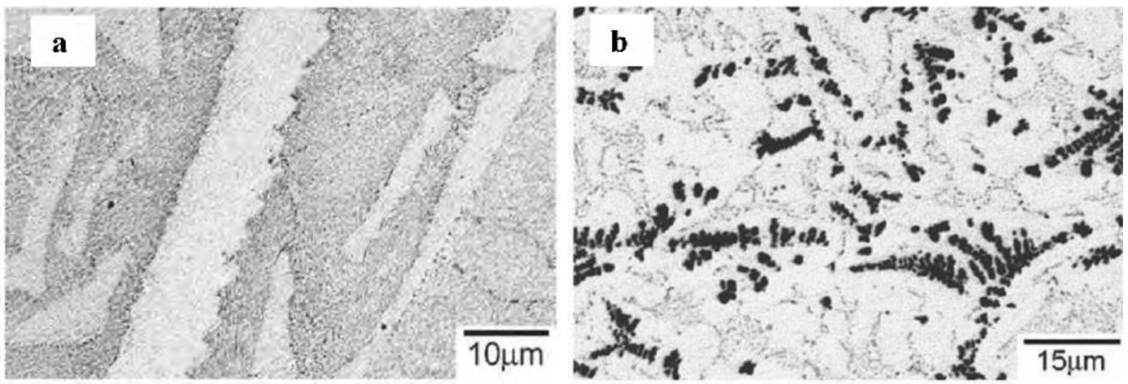

Figure 2. 2 Microstructure of Bi-Ag solder balls: (a) Bi-2.5Ag and (b) Bi-11Ag [22]

In this study, mechanical properties of the Bi-Ag alloys were correlated with the microstructural property [25], microstructures are given in Fig 2.2. Both the dendritic spacing evolution and the silver (Ag) distribution along the casting length have significant effect on the hardness. It was found that lower dendritic spacings had allowed a more widespread distribution of the Ag-rich spheroids. The higher hardness values were found connected with regions containing optimized distribution together with the lower silver content i.e.; regions close to the bottom of the casting [25]. Hardness also depends on macro segregation as well as morphology of the phases of Bi–Ag alloys.

Bi-Sb Alloy

Bi-Sb system is considered to be a non-compound forming system because of not forming IMC during soldering [26-27]. Still there is a good scope of research for developing the properties of these alloys. Bi-Sb binary phase diagram is shown in Fig.2.3.

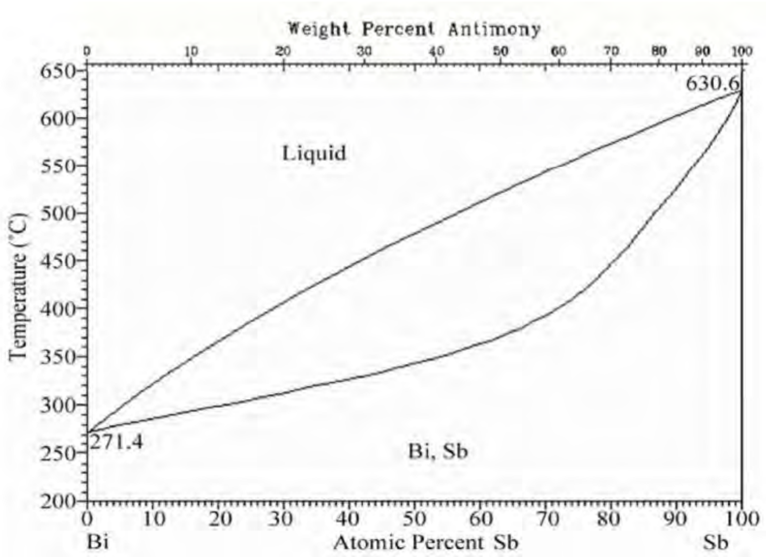

Figure 2. 3 Binary Bi-Sb phase diagram

Melting temperature of the alloy increases with increasing Sb content because of the miscibility of Sb in Bi matrix. The increasing amount of Sb increases the melting point of the solder according to the binary phase diagram of Bi-Sb alloys.

2.4.2 Au-based solder systems

Gold (Au) is considered as one of the safest elements ranked by Occupational Safety and Health Administration (OSHA) and United States Environmental Protection Agency (EPA-US) and several gold based binary and ternary alloys also fulfill solidification criteria required for high temperature soldering. Gold-based alloys have become an appropriate interconnection material in modern semiconductor and electronics industry due to desired properties [28]. Wire bonding, off wafer interconnections and flip chip technology are highly dependent on gold based alloys due to their excellent corrosion resistance, easy fabricability, good electrical and thermal conductivity,

excellent biocompatibility, nature of not forming intermetallic easily with the general solder wettable layers and simple metallurgical bond forming capacity by soldering, SLID and various other methods [28]. But, the expensive price of gold hinders its use in many potential applications. Although new horizon of opportunities for gold is being created due to rising requirements of photonics, bioelectronics and power requirements in various conventional equipment. In addition, gold can be the most demandable elements in case of smaller devices with higher functionality [28].

Au-Ge Alloy

As shown in Fig 2.4, Au–Ge is an interesting system for this application due to not having any intermetallic phases like as similar to the Pb–Sn system.

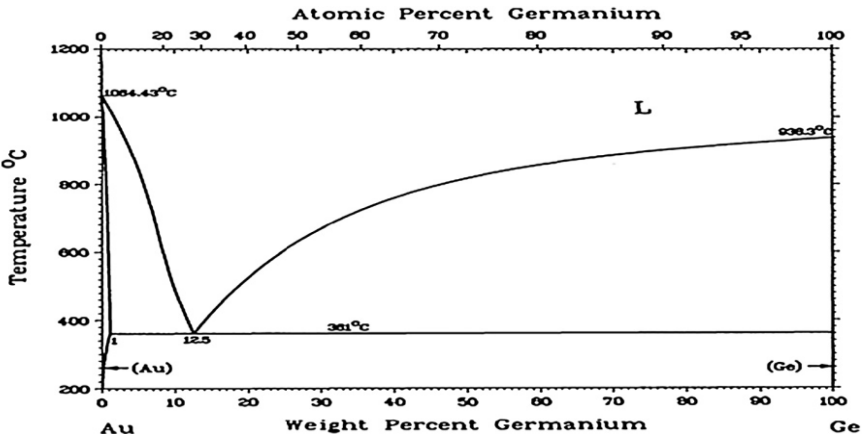

Figure 2. 4 Binary Au-Ge phase diagram [28]

The eutectic melting temperature of the Au–Ge (12.5 wt% Ge) composition is 360 °C. As the microstructures (in Fig 2.5) of Au–0.28 at% Ge alloy in both the as-cast and aged state shows the similar morphology, so the addition of Sb to the Au–Ge eutectic has a constructive effect in decreasing its melting point as well as improves its ductility substantially, despite the presence of a very hard IMC (AuSb2).

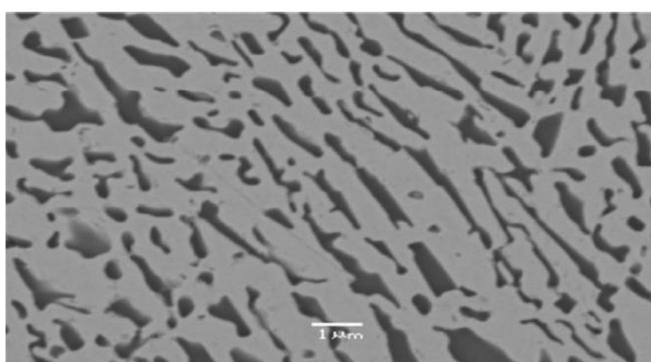

Figure 2. 5 SEM image of the as-produced Au–0.28Ge eutectic alloy showing the dark (Ge) phase dispersed on the bright (Au) matrix

The refinement of Ge phase enhances the overall increase in hardness during ageing which cannot be affected by the softening effect induced by changes in the (Au) phase [28]. The expenses associated with price of gold as well as the difficulties in electro deposition of Ge were the major problems in developing Au–Ge based candidate alloys as an alternative to high-lead content solders. The use of gold involves higher initial cost along with the potential recycling cost which in turns lowers the disposal cost. The high-temperature stability of microstructures and mechanical properties of Au–Ge based solder are extensively reported, but are limited to the bulk solder, not the solder joint, hence the interfacial reactions between the Au–Ge solder and substrate and the comprehensive properties of solder joints and their reliability over long service times should be further investigated.

Au-Sn Alloy

Gold-tin system is referred to as hard solders due to its higher stress enduring capacity comparing to the traditional soft solders such as Sn-Pb, Sn-Ag-Cu etc. The equilibrium binary phase diagram of the Au–Sn system is shown in Fig 2.6. It is a complex binary system due to the existence of four different stable intermetallic compounds with two eutectics and at least three peritectic points [28].

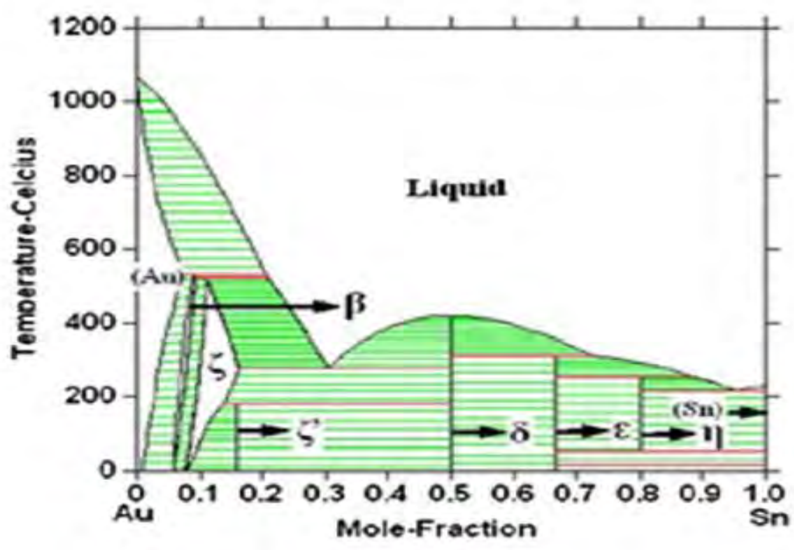

Figure 2. 6 Binary Au-Sn Phase diagram

Among the two eutectics namely Au–0.30Sn (mole-fraction) and Au–0.94Sn (mole-fraction), Au–0.30Sn is considered as high temperature solder as it has favorable melting point. The eutectic alloy becomes harder in presence of the brittle (Au_5Sn) phase. As produced Au– 0.30Sn (mole fraction) microstructure (in Fig 2.7) contains brittle ζ' (Au5Sn) and ζ (AuSn) phases dispersed in the eutectic matrix (ζ'+δ). The presence of ζ (AuSn) phase in the structure is resulted for fast cooling rate employed during the alloy production [28].

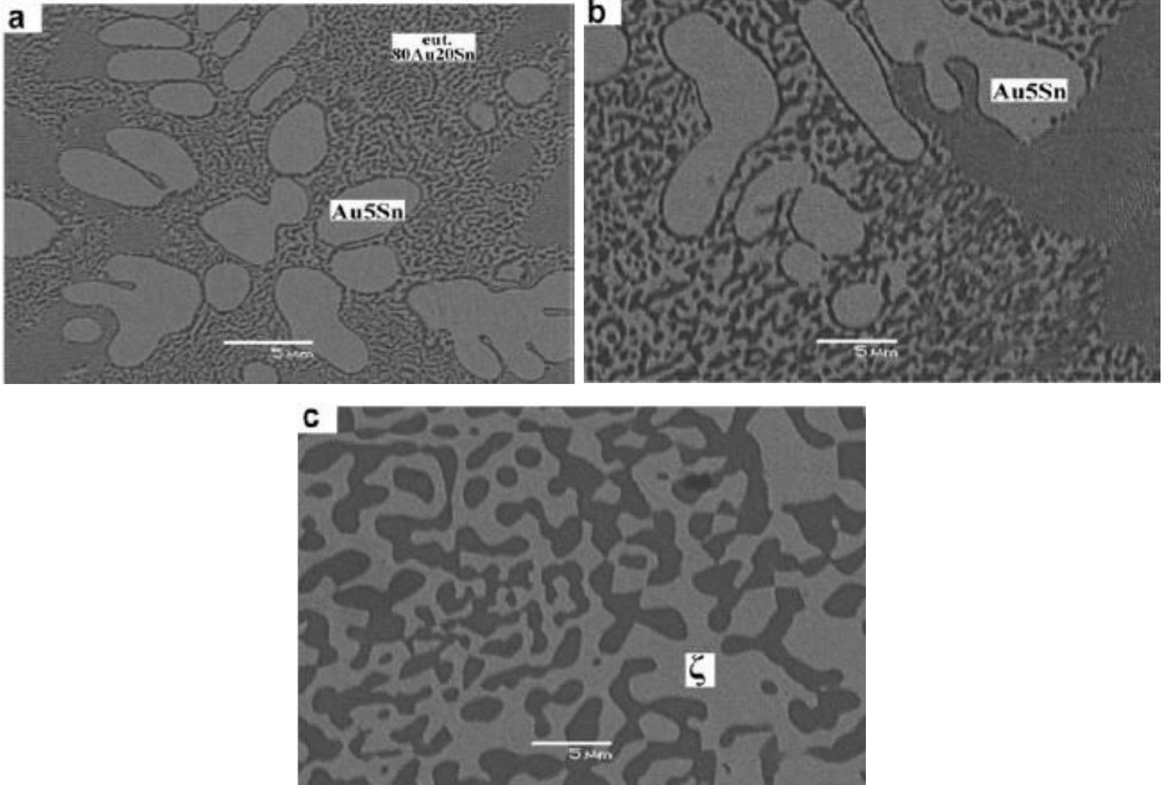

Figure 2. 7 SEM images binary eutectic Au–Sn alloy showing phase transformations during thermal aging (a) as-produced, (b) 150 °C, 1 week and (c) 200°C, 1 week

Depending on the application, these high temperature solders are generally subjected to operating temperatures ranging between 150°C to 450°C. Chidambaram et al showed in their experiment [29] that the microstructure of the Au–Sn eutectic alloy after aging at 150 °C for 1 week was comprised of large Au_5Sn intermetallic compounds (IMC) dispersed in the Au–Sn eutectic structure. The ζ phase was not present at this condition, but microstructure was comprised of ζ and δ phases after aging at 200°C. All the brittle ζ' phases are converted into ζ phases after aging at 200 °C temperature.

2.5 THE ELEMENT ZINC (Zn)

Behind the selection of Zinc as the base metal in high temperature solder alloys are the suitable properties of Zinc itself. It is referred as *spelter* in nonscientific contexts, a bluish-white, lustrous, diamagnetic metal, sometimes dull finish exists in most common commercial grades of the metal. It is somewhat less dense than iron and has a hexagonal crystal structure, is hard and brittle at most temperatures but becomes malleable between 100 and 150°C [30]. Above 210 °C, the metal becomes brittle again and can be pulverized by beating. Zn is a fair conductor of electricity, has relatively low melting (419.5°C, 787.1 F) and boiling points (907°C). Its melting point is the lowest of all the transition metals aside from mercury and cadmium.

Zn based solders are used for structural materials joining purpose for a long period. Zn has many alloys including brass, an alloy of copper and zinc, other elements to construct binary alloys with zinc are aluminum, antimony, bismuth, gold, iron, lead, mercury, silver, tin, magnesium, cobalt nickel, tellurium and sodium. While neither Zn nor zirconium is ferromagnetic, their alloy $ZrZn_2$ exhibits ferromagnetism below 35 K [31].

2.5.1 Zinc Based Solders

Zn-Mo alloy

In spite of having good thermal shock resistance properties as well as cheaper than other solder base metals, it has not been used solely due to brittleness and poor resistance to oxidation. To improve those limitations, many research have been conducted to make a high temperature Zn-based solder alloys and Zn-Mo is one of those alloys. Phase diagram of Zn-Mo is given in Fig 2.8.

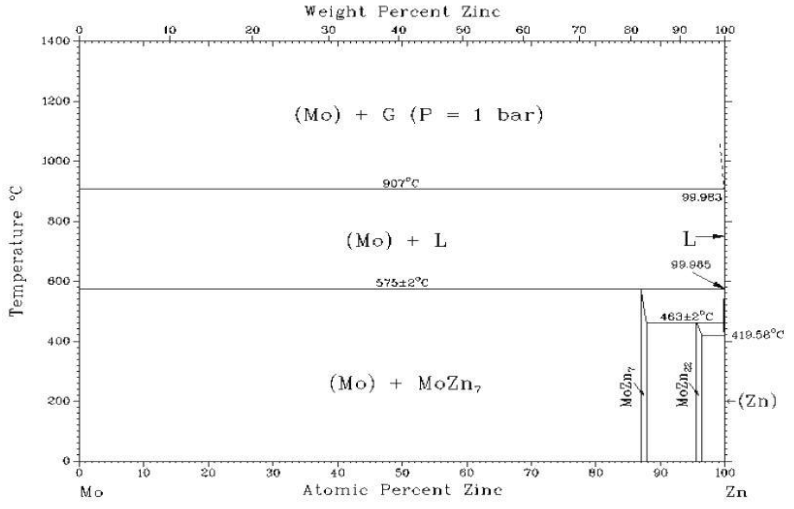

Figure 2. 8 Binary phase diagram of Zn-Mo

In relation with microstructure, as the content of Mo increases, the grains become finer drives towards the better mechanical properties. Very minute (0.4 - 0.6wt%) addition of Mo acts as nucleating agent during solidification and retards the grain growth by taking place on the boundary and formation of intermetallic compound (IMC) which leads to increased ductility, shear strength, oxidation resistance [32].

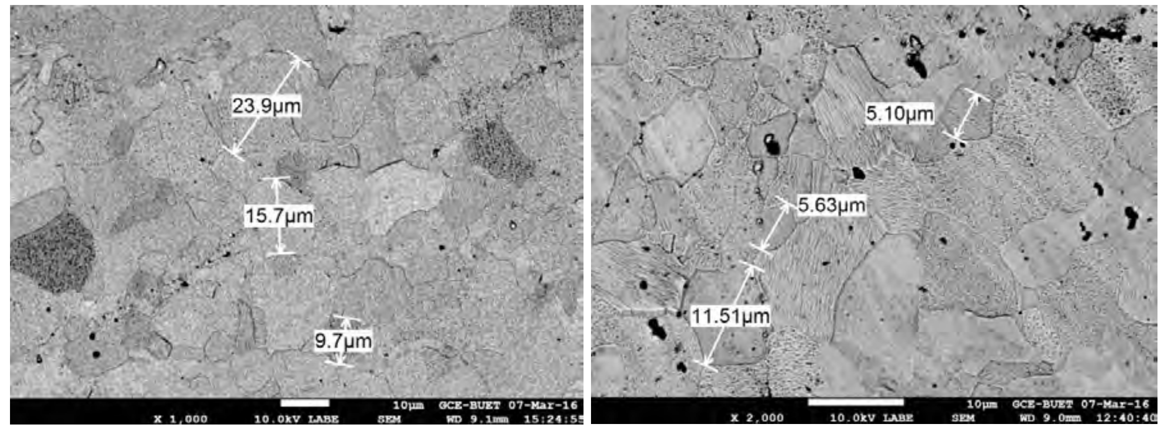

Figure 2. 9 SEM microstructures of Zn-0.4wt%Mo & 0.6wt% Mo respectively

Grain refining effect lets the hardness and tensile strength to be increased as well. But, sometimes unavailability of Mo becomes the barrier of using Zn-Mo as mainstream solder alloy.

Zn-Cr alloys

Zn-Cr binary phase diagram is shown in Fig 2.10. Similar like Zn-Mo described in earlier, grain refining was observed in line with the addition of Cr. Three alloys namely Zn-0.2wt% Cr, 0.4wt% Cr and 0.6wt% Cr were investigated with microstructure and on mechanical properties [33].

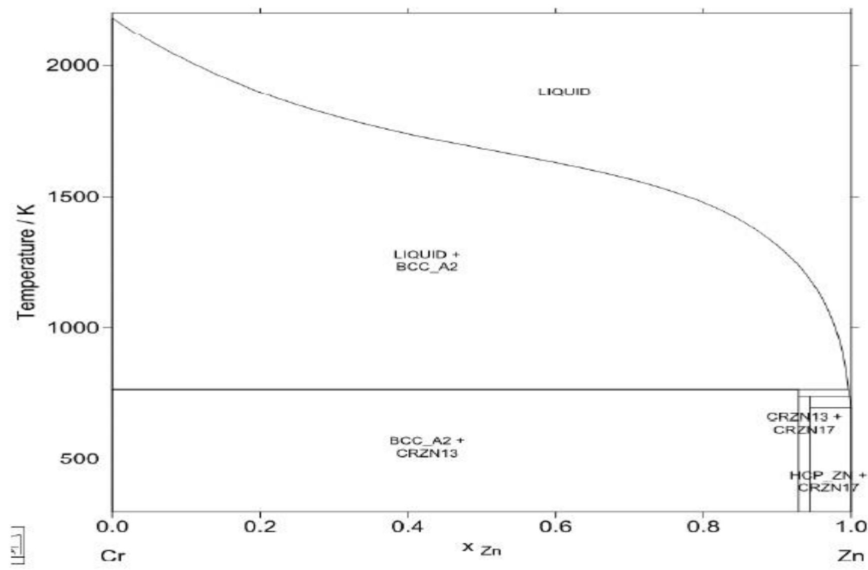

Figure 2. 10 Binary Phase diagram of Zn-Cr

Strengthening of the alloy happens with the addition amount of Cr content by precipitation in alloy and it performs dual functions such as pinning effect to the grain growth. During solidification, precipitations are formed at the grain boundaries which hinders grain growth and produces small size grains. It is evident from Hall Patch relationship that tensile strength is inversely proportional to the grain size and increases the tensile strength by pinning effect. This study also supports this theory [33].

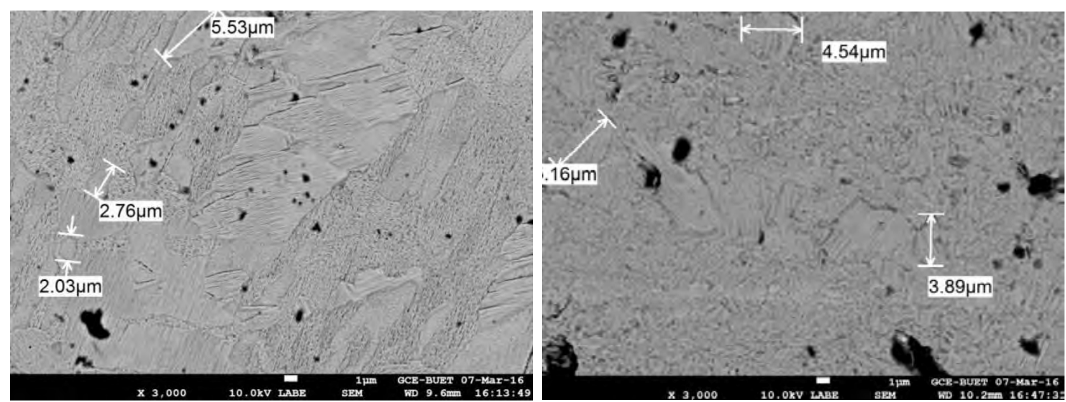

Figure 2. 11 Microstructure of Zn-0.2wt% Cr and Zn-0.4wt% Cr respectively

Dispersion strengthening is also another method in which dispersed particles of Cr precipitation obstructs the movement of dislocations. To move forward of fracture needs dislocation to be

transported from one grain to another consequences lower strength and hardness. In this study, observed higher strength might be the reason of obstructing the dislocations to move easily.

Zn-Al alloy

Major basic characteristics for being solder material are not fully existed in Aluminum which limits it to be the mainstream solder for industries and manufacturers. The conventional soldering methods have never been successful due to the tenacious aluminum oxide. The other factors like the variations of Al alloys, the dissimilarity with many solders and base metals for potential galvanic corrosion consequences; inconsistency in soldering results; and most importantly the heat acceptability of Al during soldering hinders the compatibility in solder.

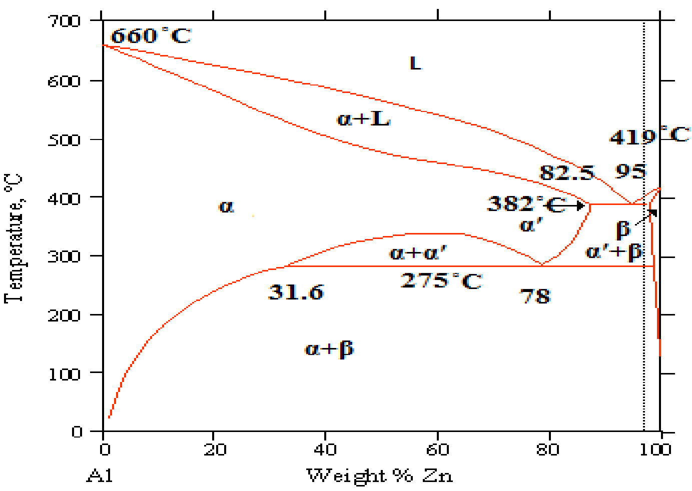

Figure 2. 12 Binary Zn-Al phase diagram [34].

Oak Ridge National Laboratory, Ford Motor Company and Johnson Manufacturing Company has demonstrated a collaborative project by using a high density infrared source of 300 kW plasma lamp to have successful results with Zn-20 wt% Al and flux at a soldering temperature of 490°C.

Figure 2. 13 Microstructure of Zn-0.3wt% Al, Zn-0.5wt% Al and Zn-0.7wt% Al respectively

From this study, higher tensile stress and fracture strain were observed as the amount of Al was increased. Mechanical tests showed that the joint area was stronger than the parent material with

minimum softening. Zn–Al based alloys have proper melting range and excellent thermal/electrical properties.

Zn-Al-Mg-Ga-Cu alloys

In this study, Zn–Al–Mg–Ga solder wire was used to attach Ti/Ni/Ag metallized Si die on Cu lead-frame in an automatic die attach machine [35]. Die attachment was performed in a forming gas environment at temperature ranging from 370 to 400 °C. At the interface with Cu lead frame, $CuZn_4$, Cu_5Zn_8 and CuZn intermetallic compound (IMC) layers were formed. At the interface with Si, Al_3Ni_2 IMC formed when 200 nm Ag layer was used at the die back and AgZn and $AgZn_3$ IMC layers when the Ag layer was 2,000 nm thick. Microstructure of the bulk solder consists of mainly two phases: one with a brighter contrast (about 80.9 wt% Zn) and another one is a mixture of light (about 73.7 wt% Zn) and dark phases (about 45 wt% Al). Die shear strength was found within the acceptable limit (21.8–29.4 MPa) for the entire die attach temperatures. In electrical test, maximum deviation of output voltage after 1,000 thermal cycles was found 12.1% [36].

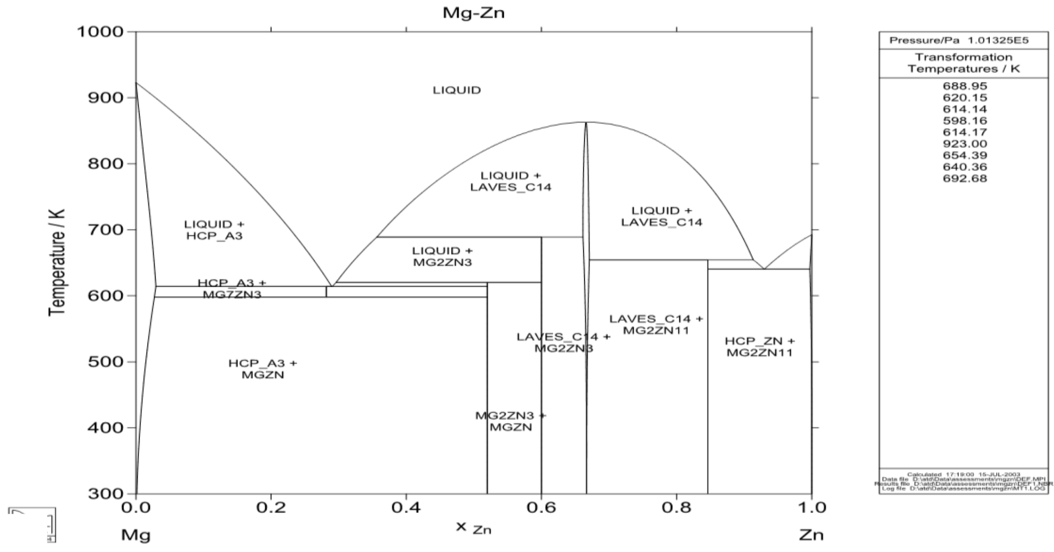

Figure 2. 14 Binary Zn-Mg phase diagram [37].

An investigation was conducted on the interfacial reactions during Si die attachment with Zn-AI-Mg-Ga high-temperature lead (Pb)-free solder on bare Cu lead-frame and Ni metallized Cu lead-frame. Cross sectional microstructural investigation revealed that as many as three intermetallic compound (TMCs) layers form at the solder/lead-frame interface for bare Cu lead-frame. Wetting on Ni metallized Cu lead-frame was found to be lower as compared to that at bare Cu lead-frame. Die shear strength was found to be higher on bare Cu lead-frame (24.2 MPa) as compared to Ni metallized Cu lead-frame (20.5 MPa).

The Zn-Al(-Cu) eutectic alloys (melting point 381°C) are candidates for use as Pb-free high-temperature solders as a substitute for Pb-based solders, which are suitable for severe working environments such as the engine room of hybrid vehicles equipped with an inverter system as well as a heat engine [38]. Interfacial reactions between Cu/Zn-4Al and Cu/Zn-4Al-1Cu with regard to the consumption of the Cu substrate, and the growth of the IMPs during soldering and aging treatments were investigated. The volume diffusion of constituent elements controlled the consumption of the Cu substrate and the growth of IMPs during soldering. In view of the aging process, the growth of IMPs is considered to be controlled by the volume diffusion. In particular, the layer thickness of c rapidly grows over 200 °C, although the thickness of βlayer grows quite slowly. With the addition of 1 mass% Cu in Zn-4Al solder, the suppressive consumption of Cu substrate was confirmed.

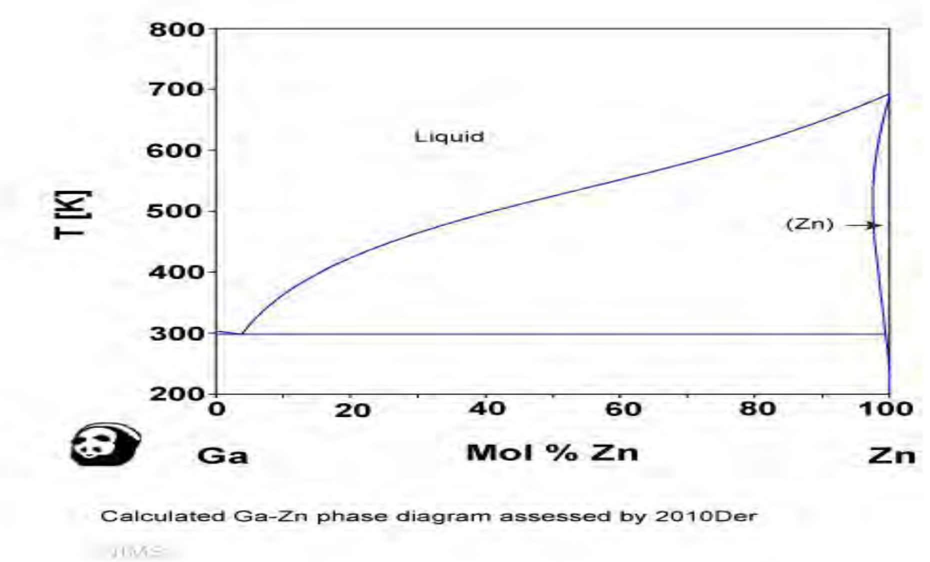

Figure 2. 15 Binary Zn-Ga phase diagram [37] .

In another study, the interfacial reaction between Zn-Al(-Cu) alloys and the Ni substrate during soldering, aging, and thermal cycling was investigated. During 420°C soldering, the Al_3Ni_2 IMC phase formed between the Ni substrate and the Zn-Al solder, the growth rate of which was very small [39]. The soldered assemblies were then heat-treated at 200°C and 300°C, where the growth of the Al_3Ni_2 remains slow. During 450°C soldering, the interfacial reaction between Ni and Zn-4Al solder proceeded continuously.

The measurements of wettability of eutectic Sn-Zn and Zn-Al alloys on the surfaces of copper and Al pads were conducted. The wettability problems discussed in other studies, resulting from the presence of ZnO or Al_2O_3 at the solder/pad interface, were eliminated by the appropriate preparation of substrates, using an appropriate flux and atmosphere, as well as the proper choice

of soldering temperature. These alloys can be used for soldering both Cu and Al. Spreading tests indicated that the wetting properties of eutectic solders based on Sn-Zn on copper pads do not depend on temperature (up to 400°C), but the solder does not wet substrate pads in less protective atmosphere. At the interface of Sn-Zn/Cu joints obtained at 250 °C, there is c-Cu_5Zn_8 phase layer as observed in other studies, and a thin strip of b-CuZn phase from the side of pad, and another thin strip of $CuZn_4$e on the side of solder.

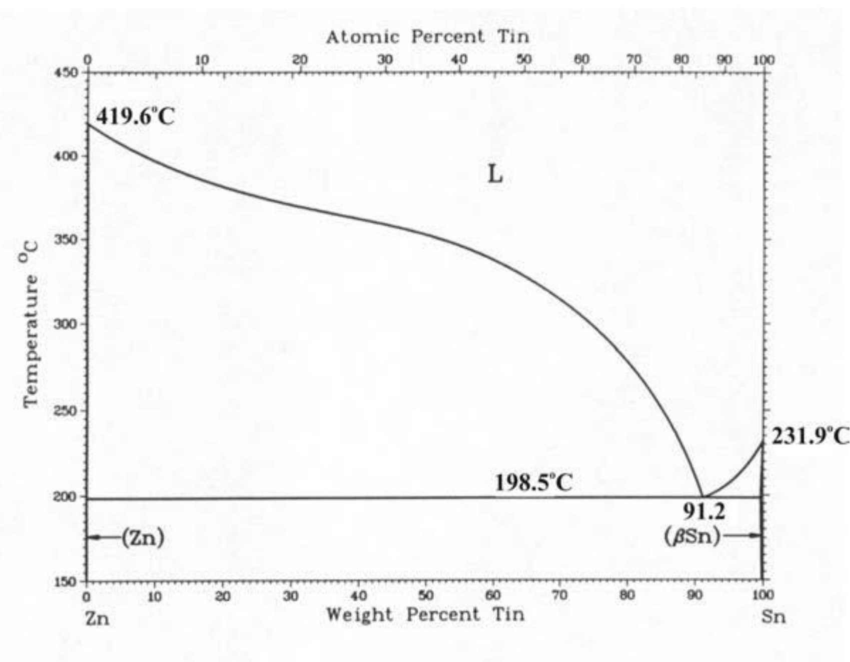

Figure 2. 16 Binary Zn-Sn phase diagram [40]

Zn-based solders were developed for ultra-high temperature applications with the alloying elements: (64–66) wt.% Al and (61–65) wt.% Cu. The solder was designed to have a liquidus temperature between 655 and 675 °K. The Al content improved the spreadability and electrical resistivity, but the Cu content had insignificant influence on the characteristics. The alloying contents increased hardness and tensile strength with the α-η eutectic/eutectoid phases. The multiple regression analysis on the measured characteristics was conducted for the alloy design of the Zn–Al–Cu solder [41].

Interfacial reaction and die attach properties of Zn-xSn solders on an aluminum nitride–direct bonded copper substrate were investigated [42]. At the interface with Si die coated with Au/TiN thin layers, the TiN layer did not react with the solder and worked as a good protective layer. At the interface with Cu, $CuZn_5$, and Cu_5Zn_8 IMC layers were formed, the thicknesses of which can be controlled by joining conditions such as peak temperature and holding time. During multiple reflow treatments at 260°C, the die attach structure was quite stable. The shear strength of the Cu/solder/Cu joint with Zn-Sn solder was about 30 MPa to 34 MPa, which was higher than that of

Pb-5Sn solder (26 MPa). The thermal conductivity of Zn-Sn alloys of 100 W/m K to 106 W/m K was sufficiently high and superior to those of Au-20Sn (59 W/m K) and Pb-5Sn (35 W/m K) [43].

The Sn-Zn-Al alloy is one of the significant alternatives for the Pb-based alloys. It is found that increasing the Zn above 10-15 wt% causes to the decrease of corrosion resistance of the alloys [44].

Recently, a new Cu-Zn alloy solder wetting layer as the Pb-free solders has been developed to reduce the IMC growth rate. The IMC growth rate on Cu-Zn layers during aging was much slower than that on Cu layers, because the Zn in the layer depressed the inter-diffusion of Cu and Sn atom.

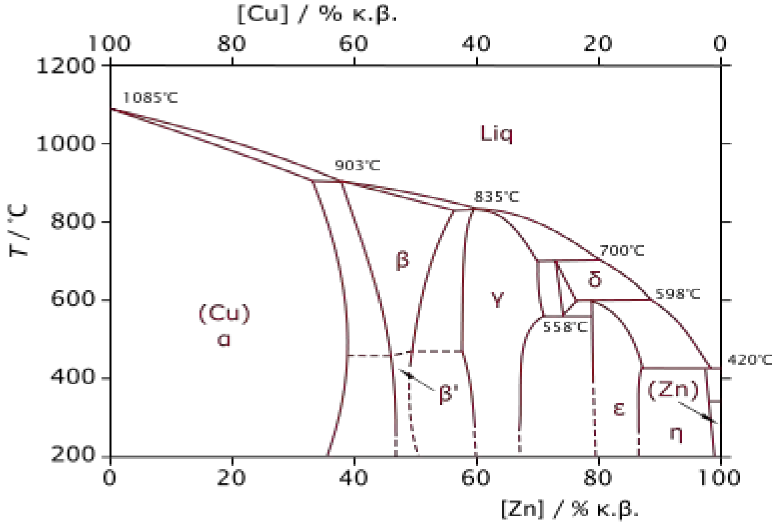

Figure 2. 17 Binary Zn-Cu phase diagram [42].

The initial shear force of as-reflowed Cu specimens was slightly higher than that of Cu-Zn specimen. The shear force of SAC solder bumps on Cu pads was slightly lower than that on Cu-Zn pads after same aging time. The drop reliability test showed the higher mean number of drops to failure of Cu-Zn specimens than that of Cu specimens both before and after aging. The enhancement of drop reliability is ascribed to the delayed growth of IMC and no micro void formation at the interfaces.

2.8 FEASIBILITY OF LEAD-FREE Zn-Sb SOLDER

Compatibility of high temperature Pb-free solders must meet the specific criteria in terms of microstructural as well as mechanical, electrical and thermal properties to be reliable for long run in high temperature applications. In contrast of the discussion in chapter 1 and above listed solder materials, feasibility based on properties can be scrutinized and summarized to the selection of appropriate high temperature solder alloy. Silver is in adequate supply but has a cost

disadvantage. Bismuth poses a potential supply problem since it is a by-product of lead mining, and also has embrittlement problems. It has also a poor conductivity both in thermal as well as electrical. Concerning cadmium, toxicity is the leading reason not to use this element. In case of Cu, there is no issue of supply, but dissolution of copper may promote growth of tin whiskers. Gallium supply and costs as well as its brittleness are the main reason not to use it. The cost, inadequate supply, poor resistance to corrosion and rapid oxide formation during melting all eliminate the element indium. Indium is safe if kept in low humidity conditions, or if it is conformably coated which demands intensive care. Tin is the base of solders, its toxicity is low and supply is adequate, but it is prone to tin pest on its own and growth of tin whiskers. Zinc is in adequate supply and toxicity is low. Antimony has an adequate history and supply to be a viable solder additive.

Now-a-days development of Zn-based solders in microelectronic packaging applications is the key interest of many researchers because of having its competitive price, proper melting range and mechanical properties [45]. The major Zn based systems researched include Zn-Ni based, Zn-Al based, Zn-Sn based and pure Zn with trace element additions [45-48]. However a complete replacement of Pb-based high temperature solders by a comprehensive analysis is yet to be made [49].

Carrying out the research on the mechanical and metallurgical analysis of Zn based die attach/solder system to give solutions to the lead-free solders, reliability problem has become the demand of time to make it scientifically worthy and to meet the industrial necessity. Addition of Sb was proven of having better microstructure stability and mechanical properties of Sn based solders. Sn-Sb solder has melting points of 235 °C to 240 °C and the melting point rises as the Sb content increases by peritectic reaction. It has not only excellent wettability and high mechanical properties at room temperature, but also an electrical resistance similar to that of Pb-Sn solders [50]. Sb does not form Sn-Sb intermetallic compound (IMC) in the interfacial reaction, moreover Sb does not affect the thickness of the intermetallic compounds (IMCs) layer for Sn based solders with substrate metallization [51]. Finally, very few researches were conducted on Zn-Sb combination, that’s why; this alloy was selected and analyzed the properties to discover a new arena in high temperature soldering applications. Among all these materials, Zn–Sb eutectic system becomes one of the most promising lead-free solders with the advantages of low melting points, excellent mechanical properties and acceptable costs.

CHAPTER 3

EXPERIMENTAL PROCEDURE

3.1 DEVELOPMENT OF NEW Pb-FREE SOLDER ALLOYS

In order to develop new Pb-free solder alloys with better performance and reliability, different amounts of pure Sb (purity 99.98%) were added with pure Zn (purity 99.99%) during casting. Three different compositions of alloy were chosen for casting to check out the mechanical behavior and characterization.

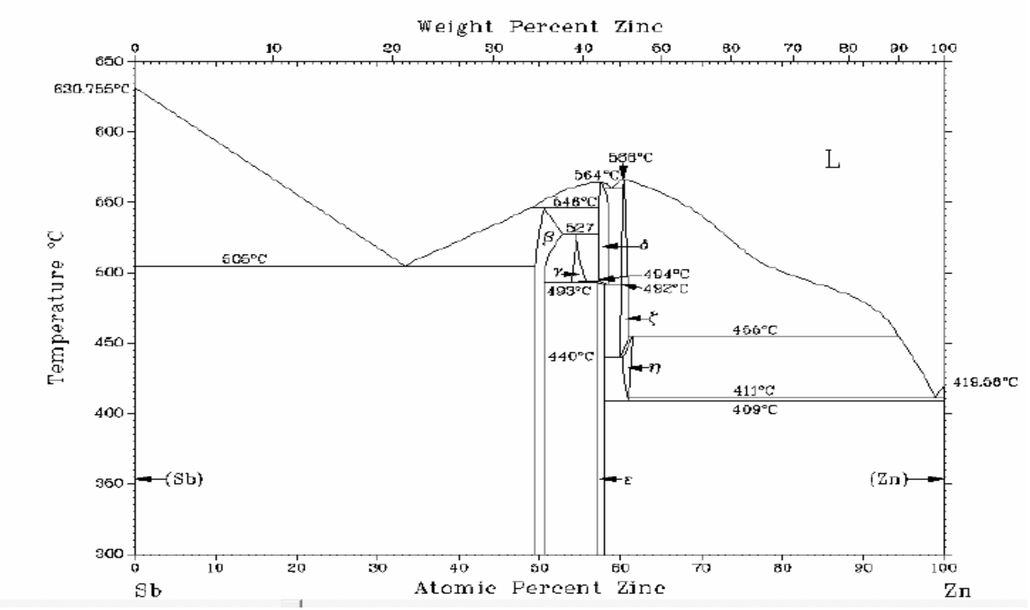

Figure 3.1 Zn-Sb phase diagram

From Zn-Sb Phase diagram (Figure 3.1), eutectic composition was found as Zn-1.7wt% Sb. Other two compositions were chosen at above and below of eutectic point as Zn-1.2wt% Sb and Zn-2.2wt% Sb. Later, alloy with better mechanical and electrical properties was selected for the ageing to observe the properties after aging at high temperature (200ºC) for two different time durations (250 hours and 500 hours). The selected compositions and ageing criteria are mentioned in Table 3.1 (a) and (b) respectively.

Table 3. 1 (a) Compositions of casted Zn-Sb alloys

Alloy Identification	Zn (Wt. %)	Sb (Wt. %)
Zn-1.2wt% Sb	98.8%	1.2%
Zn-1.7wt% Sb (Eutectic)	98.3%	1.7%
Zn-2.2wt% Sb	97.8%	2.2%

Table 3. 2 (b) Ageing information

Alloy Composition	Ageing temperature	$Time_1$ (Hours)	$Time_2$ (Hours)
Zn-1.7wt% Sb	200ºC	250	500

3.2 THE MANUFACTURE OF Pb-FREE SOLDER ALLOYS

3.2.1 Raw Materials

The Pb-free alloys were prepared from commercially pure Zn ingot (99.99%) and Sb ingot (99.98%).

3.2.2 Ingot Preparation

Before starting casting, pure Zn (melting point 419.5 °C) ingots and pure Sb (melting point 630.6 °C) were precisely weighted and record was kept for each composition. The elemental ingot of Zn was placed in a graphite crucible and kept in the gas fired pit furnace. Then temperature was raised up to 700 °C as the melting point of Sb was 630.6 °C. Next preheated Sb was added into the crucible slowly and stirred by a mechanical stirrer to homogenize the mix of metals.

Figure 3.2 Melting of Zn-Sb in Pit Furnace

Crucible was taken out of the furnace and the temperature of the molten alloy was decreased. Temperature was measured by a k-type thermocouple and recorded accordingly. At temperature 550 °C, the molten metal was poured into a preheated steel mold and cooled down to room temperature. Then metal alloy was separated from the mold. The same procedure was followed for casting of all compositions.

3.3 MATERIAL TEST AND CHARACTERIZATION OF Zn-xSb SOLDER ALLOY

These casted samples were used to prepare the samples for the following tests to know the exact mechanical, electrical and microstructural properties required to become an appropriate candidate for the replacement of toxic Pb-content solder alloys.

1. **X-ray fluorescence compositional analysis (XRF)**
   (Machine: SHIMADZU XRF-1800, USA)
2. **Microstructural analysis by Optical Microscope (OM)**
   (Machine: LEICA-MZFLIII, ITALY)
3. **Structural analysis by Scanning Electron Microscope (SEM)**
   (Machine: JEOL JSM 7600F, JAPAN)
4. **Elemental analysis of phases by EDX**
   (Machine: JEOL JSM 7600F, JAPAN)
5. **Melting behavior analysis by Differential Scanning Calorimeter (DSC)**
   (Machine: EVO 131 (SETARAM), FRANCE)
6. **Tensile Test**
   (Machine: INSTRON 3369 Universal Testing Machine, USA)
7. **Microhardness Test**
   (Machine: FV-800, FUTURE-TECH, JAPAN)
8. **Electrical Conductivity Analysis**
   (Machine: TECHNOFOUR CONDUCTIVITY METER TYPE 979, INDIA)
9. **X-Ray Diffraction analysis (XRD)**
   (Machine: BRUKER D8 advance, Germany)
10. **Creep Test by using Vickers Hardness Test Machine**
    (Machine: FV-800, FUTURE-TECH, JAPAN)

CHAPTER 4

EXPERIMENTAL ANALYSIS, RESULTS AND DISCUSSION

4.1 COMPOSITIONAL ANALYSIS

4.1.1 X-ray Fluorescence (XRF) Analysis

The prime elemental composition was confirmed by XRF analysis. The chemical compositions of the alloys are listed in Table 4.1.

Table 4. 1 Compositions in XRF are given here.

Alloy samples	Nominal Compositions (wt%)	Measured Chemical Compositions (wt%)			
		Zn	Sb	Si	Fe
Zn-1.2wt% Sb	98.8% Zn-1.2% Sb	Bal.	1.18	0.001	0.0013
Zn-1.7wt% Sb	98.3% Zn-1.7% Sb	Bal.	1.71	0.005	0.0101
Zn-2.2wt% Sb	97.8% Zn-2.2% Sb	Bal.	2.19	0.002	0.0005

It was found from the XRF analysis that Sb wt% in all alloys were almost at the expected amount. An insignificant amount of Si and Fe wt% was observed and those might be added from alloying elements and during casting as impurities.

4.2 MICROSTRUCTURAL ANALYSIS

4.2.1 Microstructure under Optical Microscope (OM) and Scanning Electron Microscope (SEM)

The chilled-cast ingots were used to study the microstructure of the Pb-free solders. The ingots were cut into a cubic sample with dimensions of 10mm x 10mm x 10mm and ground with different graded emery papers until getting finest surface followed by polishing on a non-ferrous polishing wheel using γ-alumina powder as polishing medium for about an hour for each sample until having mirror look surface. Then those samples were washed with acetone and etched with etching reagent containing 95% ethanol and 5% HCl. Finally samples were mounted in resin to make those exact horizontal and investigated the sample by optical microscope (OM) and micrographs were recorded with a digital camera (OPTIKA Microscope B-600 MET) and followed by scanning electron microscope (SEM). Also, energy dispersive x-ray (EDX) analysis was used to determine the elemental compositions at selected spots and areas. The chemical analyses of the EDX spectra were corrected by standard ZAF software.

The microstructures of the Zn-Sb alloy under Optical Microscope (OM) examination in different magnifications were given in Figure 4.1. In Figure 4.1 (a) and (b), the whitish/bright regions of

pro-eutectic Zn grain and the nucleation of eutectic phase on grain boundary were found.

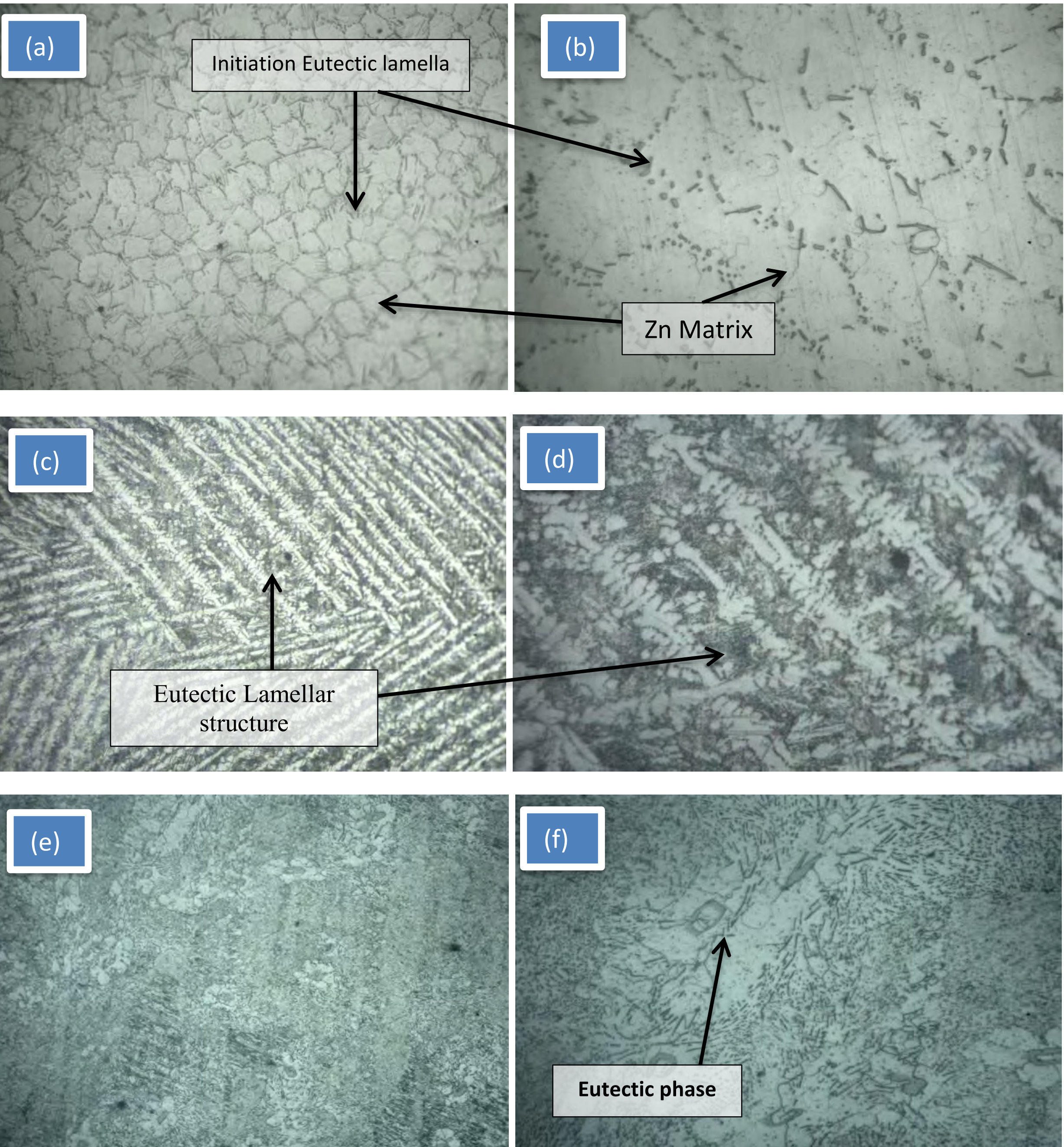

Figure 4.1 Optical micrographs of the chill-cast samples of Zn-1.2wt% Sb in (a) & (b) at 200X and 500X respectively, Zn-1.7wt% Sb (Eutectic) in (c) & (d) at 200X and 500X respectively, Zn-2.2wt% Sb in (e) & (f) at 200X and 500X respectively

Figure 4.1 (c) & (d) exhibited the eutectic lamellar microstructure (ε-Sb_3Zn_4+Zn) of eutectic Zn-1.7wt% Sb distributed throughout the whole matrix and indicated the complete dissolution of Sb in Zn. As the amount of Sb was increased to 2.2 wt%, the morphology was observed consisting the increasing number of intermetallic compound (IMC) while eutectic phase was decreased and at the same time IMC size became larger as shown in Figure 4.1 (e) & (f).

The microstructures of Zn-xSb alloys were also examined under Scanning Electron Microscope-SEM in the Back Scattered Electron (BSE) mode, as displayed in Figure 4.2 a-c and in Secondary Electron Imaging (SEI) mode in Figure 4.3 a-c. The structure clearly revealed the matrix of Zn constituting the nucleation of eutectic phase in Figure 4.2 (a) and 4.3 (a). It was observed that, with increasing the amount of Sb content in the alloys, the grains of the alloys became finer. This grain refining behavior due to addition of Sb had a significant effect on the mechanical, electrical and other characteristics of the solder alloys. Sb particles were found to be dispersed in the whole structure, leading to the eutectic Zn-1.7wt% Sb in Figure 4.2 (b) and 4.3 (b). Secondary Electron Images (SEI) were also observed in SEM which is given in Figure 4.4 a-c.

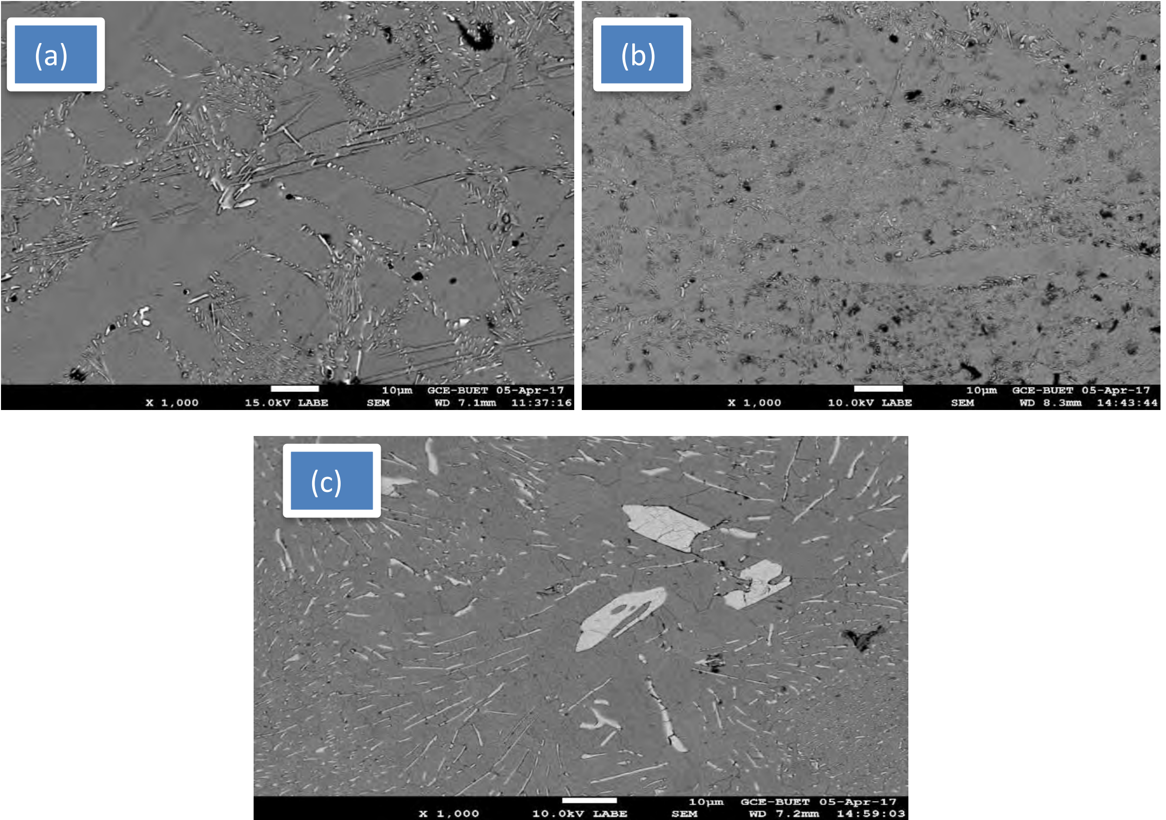

Figure 4. 2 SEM microstructure in BSE mode of chill-cast samples of (a) Zn-1.2wt% Sb, (b) Zn-1.7wt% Sb (Eutectic), and (c) Zn-2.2wt% Sb (all images taken at 1000 X).

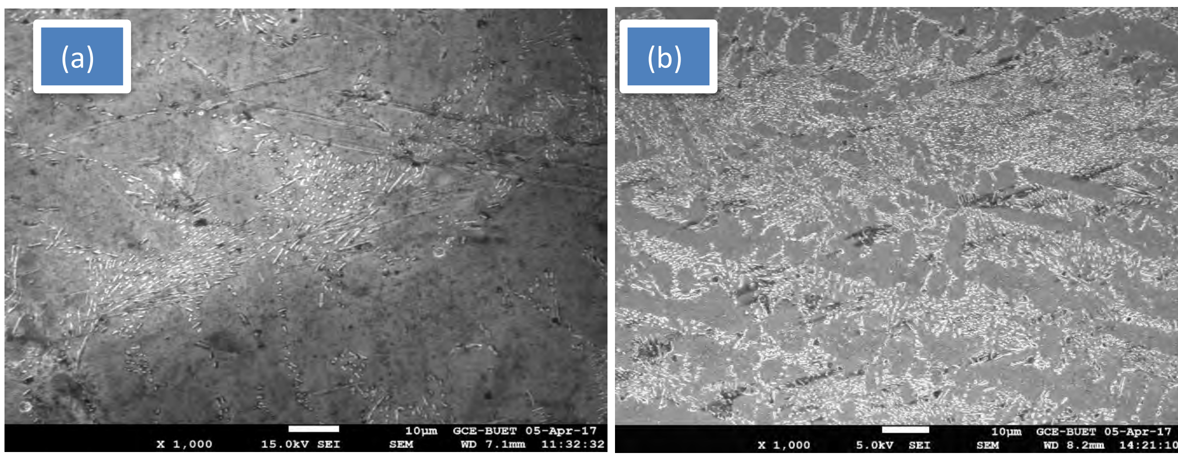

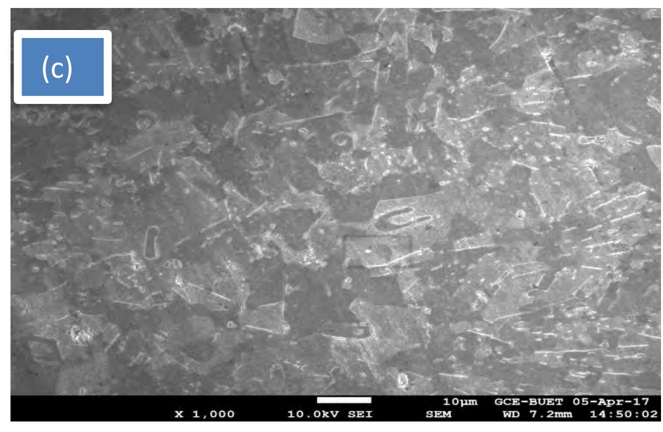

Figure 4. 3 SEM microstructure in SE mode of chill-cast samples of (a) Zn-1.2wt% Sb, (b) Zn-1.7wt% Sb (Eutectic), and (c) Zn-2.2wt% Sb (all images taken at 1000 X).

4.2.2 Energy Dispersive X-ray (EDX) analysis

It was clear from the above discussion that addition of Sb effectively changed the microstructure of Zn-xSb solder alloys. In order to analyze the distribution of different elements in different phases, EDX analysis was used to determine the elemental composition at selected areas and spots of Zn-xSb alloy.

003 VFS=10203 count

Element	(keV)	Mass%	Sigma	Atom%	Comp
O K	0.525	0.44	0.03	1.78	
Zn K	8.630	99.56	1.78	98.22	
Sb L					
Total		100.00		100.00	

004 VFS=9873 count

Element	(keV)	Mass%	Sigma	Atom%	Comp
O K	0.525	0.61	0.02	2.47	
Zn K	8.630	97.86	0.92	96.72	
Sb L	3.603	1.53	0.18	0.81	
Total		100.00		100.00	

Figure 4. 4 SEM microstructure of chill-cast Zn-1.2wt% Sb with EDX spectrum at point 3 presenting 100 wt% Zn & point 4 consists eutectic composition.

In Figure 4.4, EDX spectrum and composition in the former point exhibited the pro-eutectic Zn phase with composition approximately 100 wt% whereas latter one showed the nucleation of eutectic structure on the grain boundary.

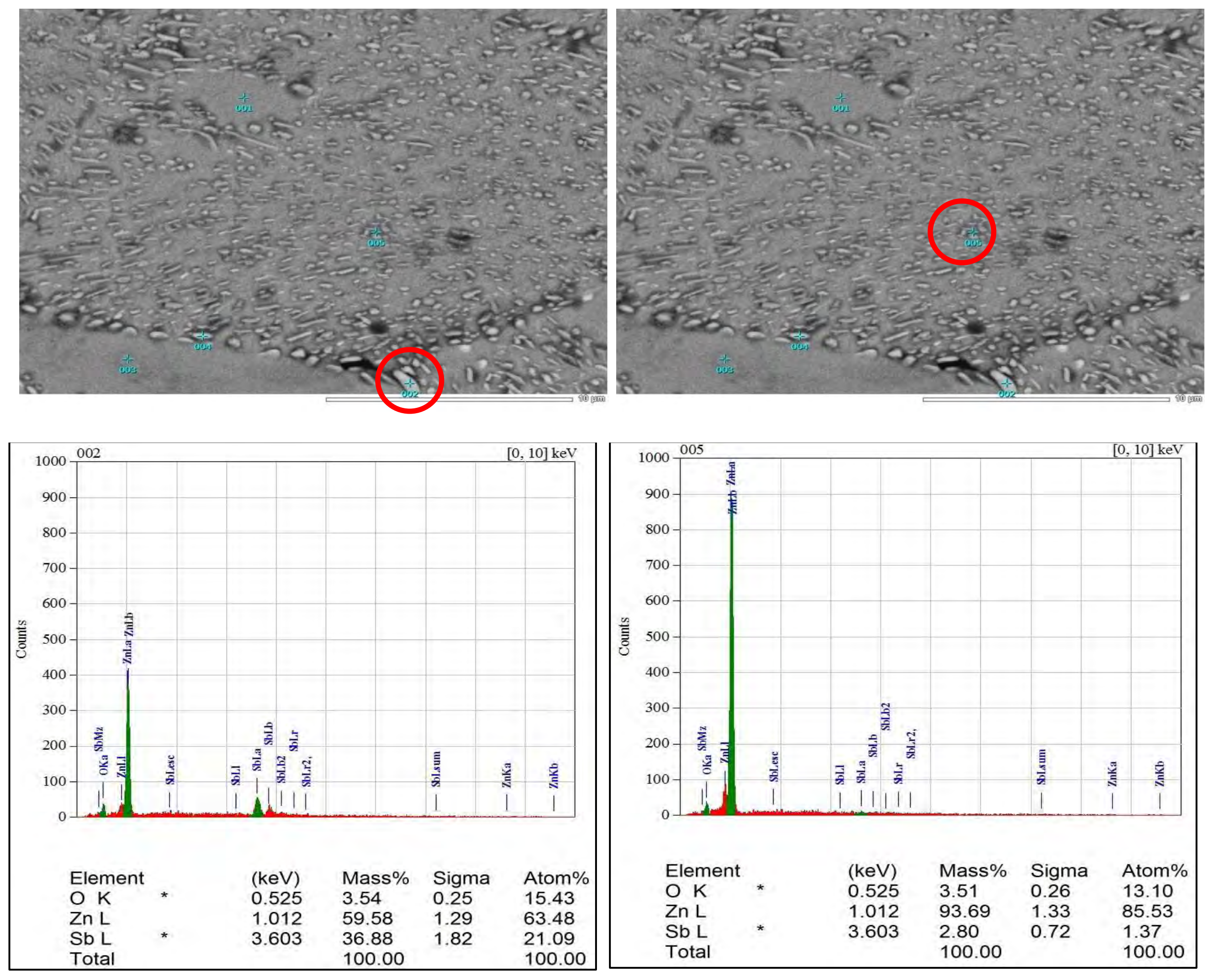

Element		(keV)	Mass%	Sigma	Atom%
O K	*	0.525	3.54	0.25	15.43
Zn L		1.012	59.58	1.29	63.48
Sb L	*	3.603	36.88	1.82	21.09
Total			100.00		100.00

Element		(keV)	Mass%	Sigma	Atom%
O K	*	0.525	3.51	0.26	13.10
Zn L		1.012	93.69	1.33	85.53
Sb L	*	3.603	2.80	0.72	1.37
Total			100.00		100.00

Figure 4. 5 SEM microstructure of chill-cast eutectic Zn-1.7wt% Sb with EDX spectrum.

Whitish particle at point 2 (first picture) in Figure 4.5 contained the ε-Sb_3Zn_4 phase with 60 wt% Zn and 37 wt% Sb and 3wt% O was also present which might be added during exposure of the alloy to the air. Latter microstructure in Figure 4.5 showed clear lamellar structure with near about the eutectic composition.

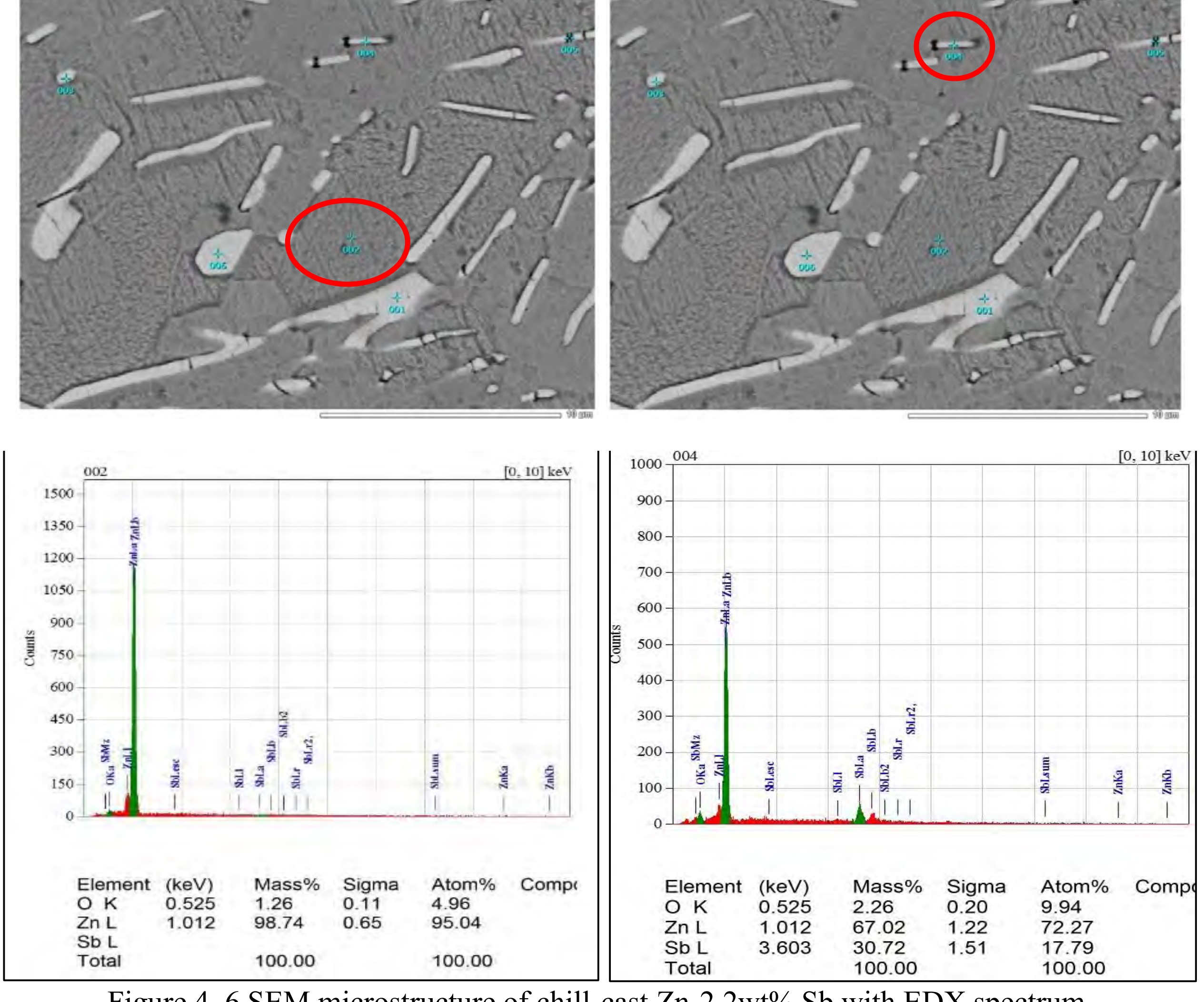

Figure 4. 6 SEM microstructure of chill-cast Zn-2.2wt% Sb with EDX spectrum.

The grey colored matrix marked in first red circle in first spectrum of Figure 4.6 consisted of mainly Zn matrix with 99 wt% Zn and balance was some oxide, whereas the Sb-rich whitish planner rod like IMC consisted of 67 wt% Zn and 31 wt% Sb, corresponding to the stoichiometry of ε- Sb_3Zn_4 phase at point 4 in Figure 4.6.

4.3 ANALYSIS ON THERMAL AND MECHANICAL PROPERTIES

4.3.1 Introduction

Modern electronic assemblies are made up from materials with a wide range of thermal expansion coefficients. When an electronic device is in operation, it normally generates heat. As these materials are packaged together in the device, internal thermal stresses and strains will result under temperature excursions during operation. This is why one of the main focuses in material selection for electronic assembly is to provide the least amount of thermal mismatch. However, in practice, this cannot be fully achieved and the thermal stresses in an assembly are unavoidable. It

is therefore important for solder alloys, as prime interconnection materials, to be able to withstand the high thermal stresses. It is also known that the absolute operating temperature, T_{op}, is very close to absolute melting temperature, T_m, of the solder. As a result, the homologous temperature, ($\eta=T_{op}/T_m$), is usually greater than 0.6 when the assembly is operated at room temperature. Hence, the solder material is normally subjected to creep during operation even at room temperature due to high stress. This means that the Pb-free solders should have their melting point low enough to be comparable with that of Sn-37Pb and as well as high enough for the solder joint to bear the operating temperatures. Besides, the Pb-free solders should have and retain adequate mechanical strength such as tensile and creep resistance during their operation. As the mechanical strength and melting behavior of solder alloys are important for a successful solder alloy, this chapter discusses mainly these issues.

4.3.2 Melting Behavior Analysis

Soldering, a joining process of two substrates, is a very important technique in the packaging of electronic products. As per the temperature profile of the reflow furnace, the solders are first heated up, then become molten, reacted with the substrates; cool down, and lastly solidify. The temperature profile of the reflow furnace is the key process controller for obtaining a good assembly. Insufficient heating can result in non-wetting at the solder joint, whereas excessive heating introduces enhanced interfacial reactions and possible reliability problems [52]. Low cycle thermal fatigue is known as the foremost failure mode in case of solder joints caused by the mismatching of thermal expansion between the jointed components and heat dissipation from devices during operation [53]. The knowledge of melting and solidification characteristics of solders is crucial in the selection of the temperature profile for the reflow furnace.

A differential scanning calorimeter (DSC) was used in the present study to determine the melting and solidification characteristics, such as the onset temperatures of phase transformation and the enthalpy of fusion of the different Pb-free alloys. The heating rate for the DSC test was 5^0C/min in nitrogen atmosphere. The temperature range was from 30^0C to 600^0C during the analyses. The first onset temperature was the temperature at which the sample begins to melt, and was regarded as the solidus line [54]. The peak temperature was reached at the end of melting range of sample, and was regarded as the liquidus line. So the DSC was used to find the melting temperature and as well as the melting range of Pb-free Zn-Sb solder alloy.

Figure 4.7 (a) shows the DSC curve for the eutectic Zn-1.2wt% Sb alloy and the melting temperature was observed at 416.50 °C and the same in Figure 4.7 (c) shows 419.67 °C for Zn-2.2wt% Sb alloy.

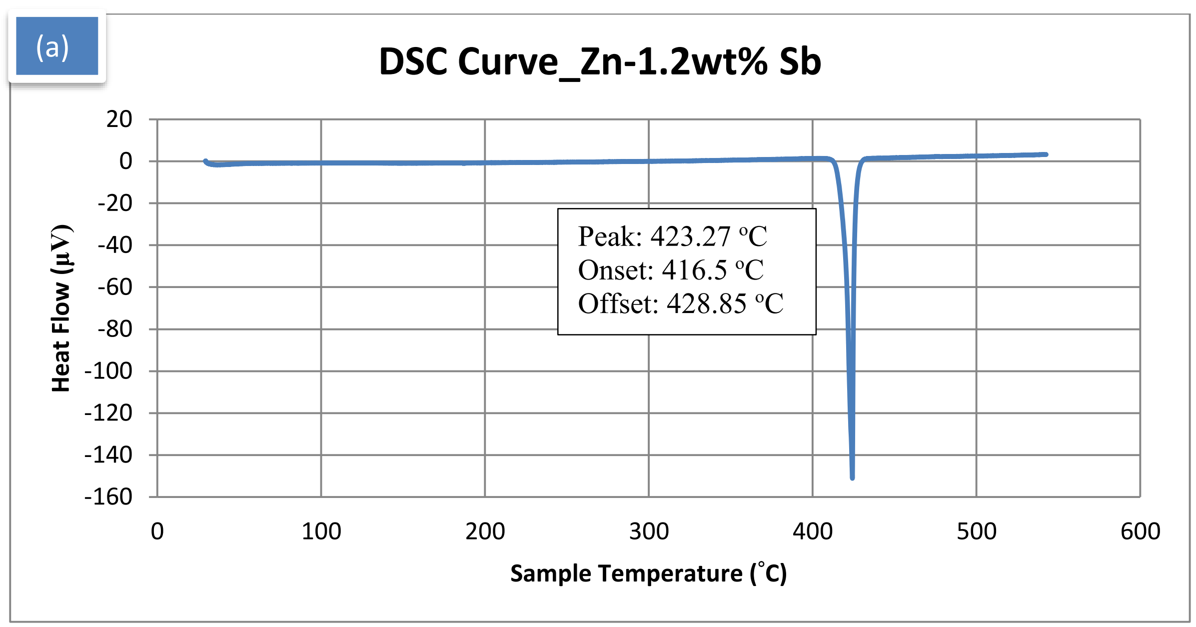

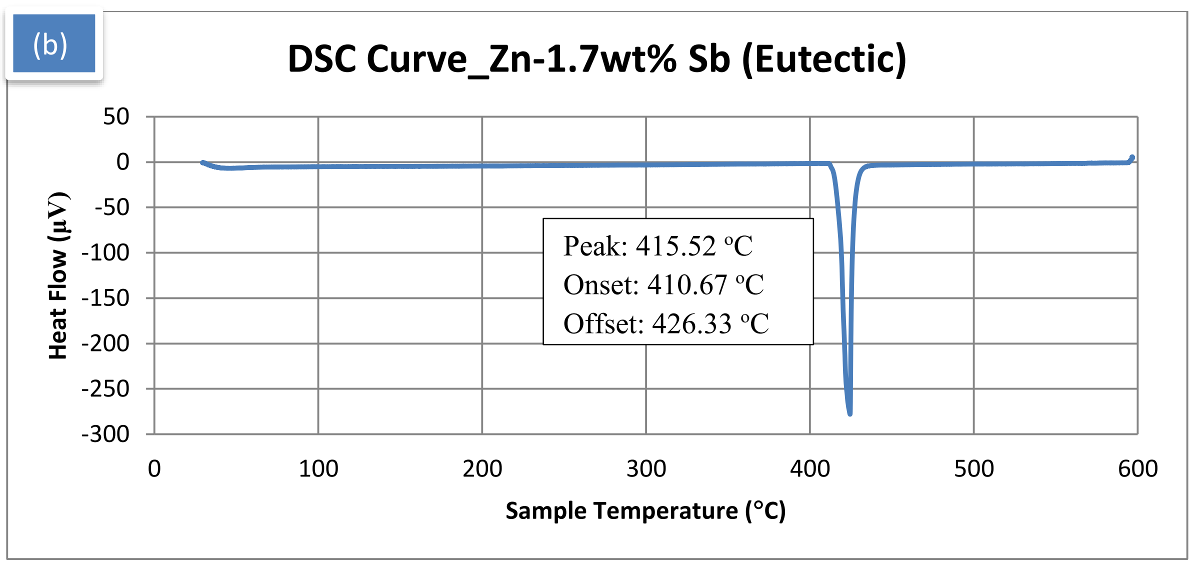

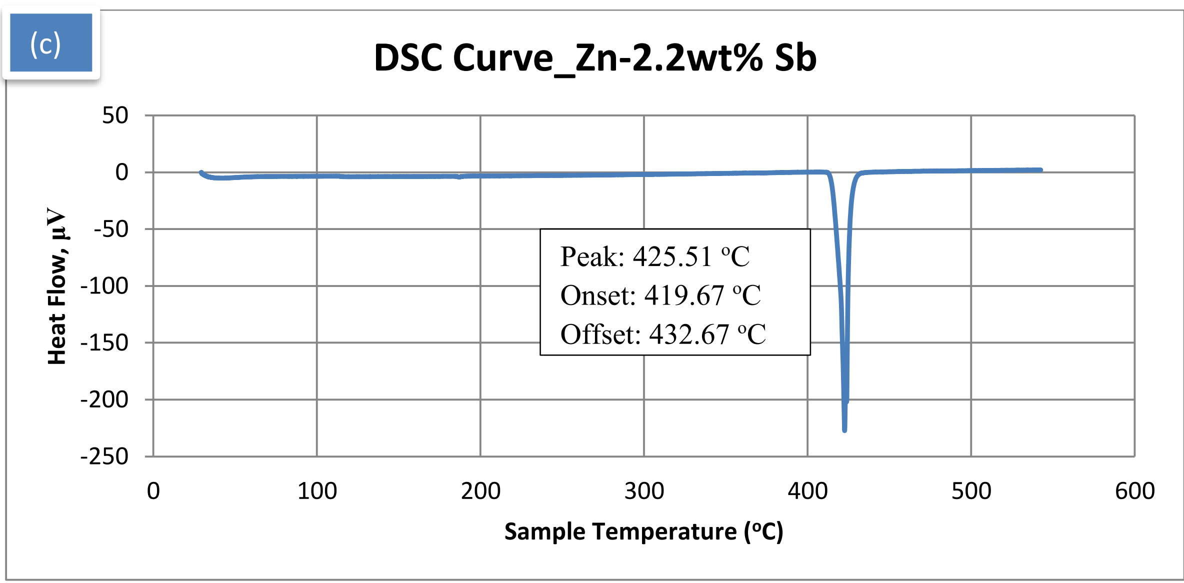

Figure 4. 7 The DSC curves on heating of (a) Zn -1.2wt% Sb, (b) Zn -1.7wt% Sb (c) Zn -2.2wt% Sb [Appendix A]

But, the DSC curve for Zn-1.7wt% Sb eutectic alloy in Figure 4.7 (b) exhibited the melting temperature at 410.67 °C (eutectic melting point 411 °C) which was considerably lower than the other two alloys. As solder alloy should have lower enough melting temperature to avoid thermal damage to the assembly being soldered and to avoid creep behavior, so the eutectic Zn-1.7wt% Sb with lowest melting point among these three alloys can be an appropriate competitor in replacing Sn-xPb solder alloy. Table 4.2 shows the melting and liquidus temperature for different solder alloys.

Table 4. 2 Melting and Liquidus Temperature for different solder alloys

Material	Melting Temp, ºC	Liquidus Temp, ºC
Zn-1.2wt% Sb	416.50	423.27
Zn-1.7wt% Sb	410.67	415.52
Zn-2.2wt% Sb	419.67	425.51

4.3.3 Microhardness Test

The prime characterization of mechanical properties of any solid-state surfaces is the measurement of hardness, especially microhardness. This is often considered as the resistance of the material to abrasion or wear. Durability during use and suitability for special applications of any material can be confirmed by its Hardness. The method of testing had been set to determine the hardness of individual grains, phase and structural component of alloys since it's more sensitive to the microstructure of the solder than its chemical composition. The motion of dislocation growth and configuration of grains mostly control the microhardness of a solder alloy. Therefore, the mechanical property such as the microhardness depends especially on the microstructure, processing temperature, the composition and so on [55]. The microhardness measurement in the present study was performed on the samples using a Vickers Shimadzu microhardness tester. Before indentation testing, necessary grinding and polishing were done to obtain a polished, smooth and flat parallel surface. The applied load was 1 kg for 10s and 7-10 readings of different indentation were taken at room temperature to obtain the mean VHN value.

The hardness can be calculated from the equation which is given below;

$$VHN=1.854P/d^2$$

Where,

P=applying load (1 kg)

d=diagonal length of the indentation.

The results obtained of the microhardness at small load of the Zn-1.2wt% Sb, Zn-1.7wt% Sb and Zn-2.2wt% Sb solder alloys were presented in Figure 4.8. [Appendix B]

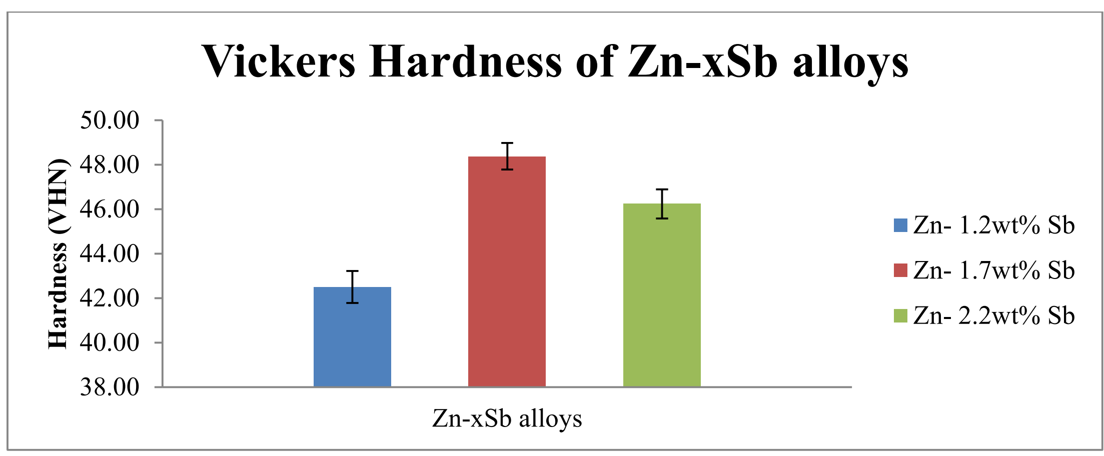

Figure 4. 8 Microhardness values in terms of Vickers Hardness Number for different Zn-xSb solder alloys.

Since Sb has the strengthening effect on pure Zn and make the grains finer in microstructure of eutectic alloy than pro-eutectic Zn-1.2wt% Sb, so hardness was also found higher in eutectic alloy accordingly. As shown in Figure 4.8, hardness was increased with increasing of Sb until Zn-1.7wt% Sb eutectic alloy, but it was decreased in Zn-2.2wt% Sb due to the formation of large Intermetallic Compound (IMC) which consumed more Sb from the original matrix and weakened the whole alloy [56-57]. Vickers Hardness Number (VHN) of Zn-1.2wt% Sb alloy was found 42.5 whereas it was increased in Zn-1.7wt% Sb to 48.38 and but it was 46.24 in Zn-2.2wt% Sb. So the highest hardness number was found 48.38 in eutectic alloy which is also way higher than 12.20 found for mostly used 63Sn-37Pb solder alloy [58-59].

4.3.4 Tensile Test

The ultimate tensile strength (UTS) is the maximum engineering stress, which a material can withstand in tension, on the engineering stress-strain curve [60]. The yield stress is the stress level at which plastic deformation begins. For solder alloys, the yield stress is commonly defined by the stress on the stress-strain curve at 0.2% strain offset. It is also called the 0.2% proof stress.

The tensile specimens were prepared by the mechanical machining of chill-cast ingots. They had a gauge length marked 25.00mm for each samples, the width and thickness for each samples were 6.00mm and 5.00mm respectively as shown in Figure 4.9. Tensile tests were carried out on an Instron testing machine at a rate of 1.00mm/min at 298K to obtain data on the stress-strain curves which contained information of elongation at fracture and the UTS.

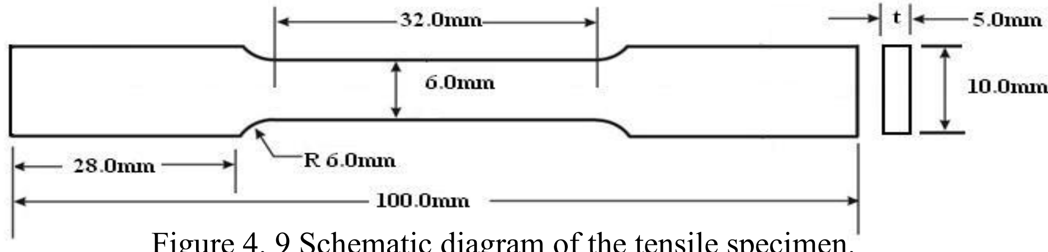

Figure 4. 9 Schematic diagram of the tensile specimen.

With the addition of Sb in Zn, it was expected of improving its mechanical properties due to the modification of the microstructure as mentioned in the previous chapter.

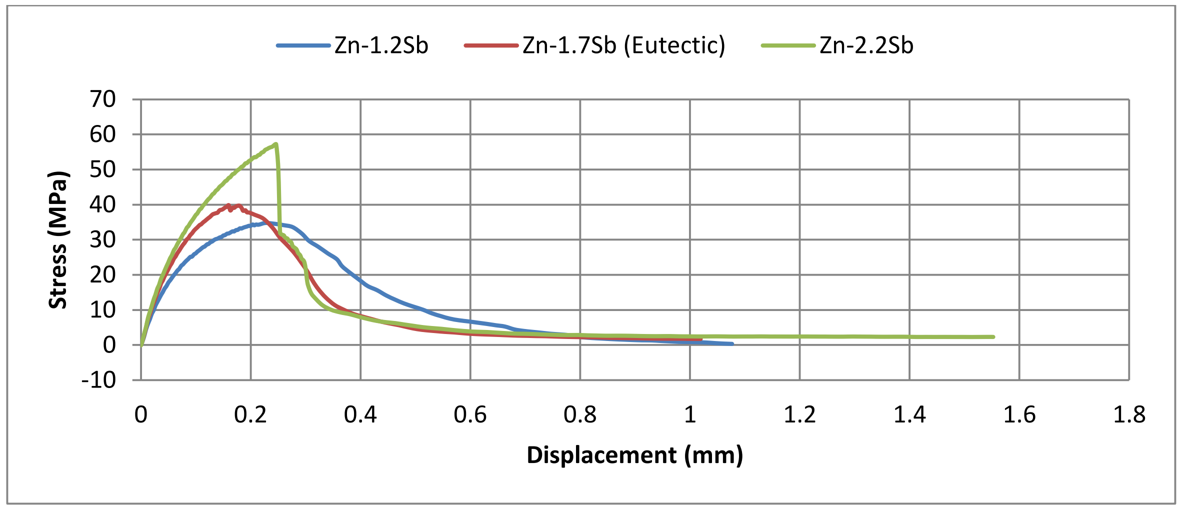

Figure 4. 10 Tensile stress-strain curves of Zn-1.2wt% Sb, Zn-1.7wt% Sb, and Zn-2.2wt% Sb solder alloys. [Appendix C]

Figure 4.10 shows the typical stress-strain curves of Zn-1.2wt% Sb, Zn-1.7wt% Sb, and Zn-2.2wt% Sb solder alloys. Both Yield Tensile Strength (YTS) and Ultimate Tensile Strength (UTS) were observed higher in Zn-1.7wt% Sb eutectic alloy than those of Zn-1.2wt% Sb. On the other hand, both properties for Zn-2.2wt% Sb were higher than the other two alloys, but at UTS point, load dropped sharply and failed the alloy immediately after reaching peak point. It indicated that Zn-2.2wt% Sb was hard but brittle and had very limited ductility. Among these three alloys, the eutectic Zn-1.7wt% Sb exhibited the optimum strength with appropriate elongation and ductility. An increase in 2% of the proof strength was observed for addition of 1.7 wt% Sb in Zn, as well as a 10% drop in elongation was observed for the same. Contrasting with tensile strength (52.49 MPa) and elongation (41.62%) of mostly used 63Sn-37Pb solder alloy, both were found slightly lower (40 MPa and 38%) for 1.7wt% Sb [58].

Table 4. 3 Mechanical properties of Zn-1.2wt% Sb, Zn-1.7wt% Sb and Zn-2.2wt% Sb [Appendix C]

Alloys	Melting point, (ºC)	Micro hardness, (VHN)	Tensile Strength, (MPa)	Elongation, (%)
Zn-1.2wt% Sb	416.50	42.50	35	42
Zn-1.7wt% Sb	410.12	48.38	40	38
Zn-2.2wt% Sb	419.67	46.24	57	6

Table 4.3 shows the melting, tensile and hardness properties of Zn-1.2wt% Sb, Zn-1.7wt% Sb and Zn-2.2wt% Sb solder alloys. Considering the above properties, the eutectic alloy Zn-1.7wt% Sb hold the desired characteristics and appropriate as the solder alloy.

4.3.5 Electrical Conductivity Analysis

Electrical conductivity is a measure of a material's ability to conduct an electric current. It was determined in this experiment in %IACS (International Annealed Copper Standard) conductivity. The resistivity and conductivity can be calculated from the following formulae by using % IACS formula: Resistivity= 172.41/ %IACS conductivity [61-62].

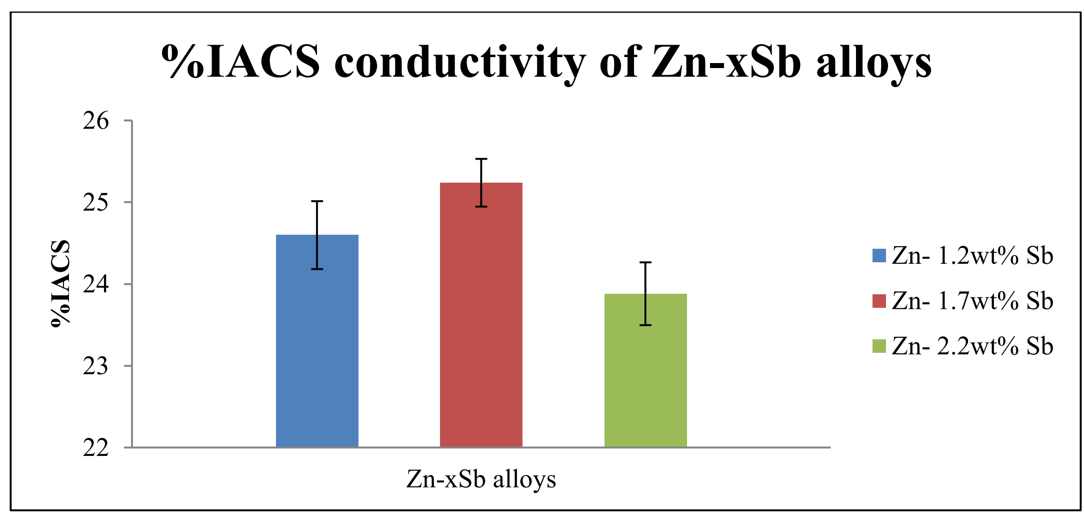

Figure 4. 11 %IACS of Zn-1.2wt% Sb, Zn-1.7wt% Sb and Zn-2.2wt% Sb

The electrical resistivity of Zinc is 59.0 nΩ·m (at 20 °C) while the same of Antimony is 417 nΩ·m (at 20 °C) [63]. Sb has tendency to restrict the electrical current more than Zn resulting lower conductivity as the Sb% increases in Zn. But it contradicted in the above experiment result shown in Figure 4.11, the %IACS of Zn-1.2wt% Sb is 24.60 whereas it was found higher 25.24 for Zn-1.7wt% Sb because of lamellar fine microstructure. In case of Zn-2.2wt% Sb pro-eutectic alloy, conductivity was reduced to 23.88 which was lower than that for both Zn-1.2wt% Sb and eutectic Zn-1.7wt% Sb alloys and it followed the theory. Conductivity of Zn-1.7wt% Sb alloy (25.24) was also found much better contrasted with the same (11.89) of 63Sn-37Pb [64]. So, having better electrical properties like conductivity placed it way ahead to a good extend in selecting the Pb-free high temperature solder alloy.

4.3.6 X-ray Diffraction (XRD) Analysis

X-ray diffraction (XRD) technique was used to identify the phases present in the alloy samples and to confirm of presence of any intermetallic compound formed in the alloy. This analysis was carried out by using a Bruker D8 advance machine. Square sized samples with 10 mm breadth and 2 mm thickness were used for XRD. To inspect the presence of phase, Cu-Kα radiation with wavelength of 0.15418 nm was used and the line counts were plotted against the diffraction angle 2θ starting from 10° to 90° with an increment of 0.02°. The obtained peaks at different 2θ position were analyzed with the standard available for the same experimental condition.

XRD was performed in order to identify the phases and the XRD pattern of Zn-xSb alloys was depicted in Figure 4.12. PDF 2 software was used to analyze the whole pattern and searched for any intermetallic or any other phases comprising of Zn/Sb.

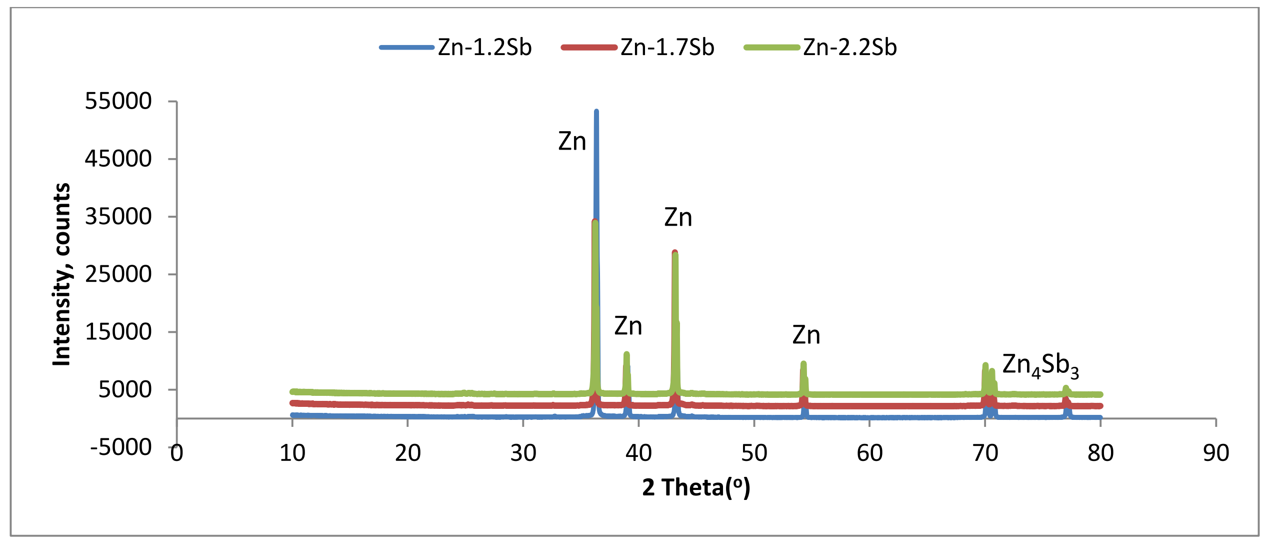

Figure 4. 12 XRD peaks of Zn-xSb alloys.

The peaks pattern obtained here in case of alloys showed in Figure 4.12 have similarity with that of pure Zn and Zn_4Sb_3, only slightly differ in position (around 2 theta= 0.02-0.08 degree). However, the slight shifting of the prominent peaks was occurred due to the presence of these particles in the pure Zn. Peaks located at 37°, 37°, 43° and 54° confirmed the characteristics of Zn. Furthermore, peaks for Zn_4Sb_3 were also found at 71° and 77°. So, XRD analysis verified the phases in the alloys taken for this research.

4.3.7 Creep Behavior Analysis

Creep is the long term deformation propagating slowly in solid materials and may cause permanent failure under the influence of high mechanical stresses and temperature. It is also sometimes called as cold flow. Long-term exposure to high levels of stress and temperature mainly results creep in the material even that stress is still below the yield strength. Since creep deformation spreads very slowly upon the application of stress and heat unlike brittle fracture and strain accumulates as a result of long-term stress, therefore creep is termed as the "time-dependent" deformation.

The results obtained for the hardness, H, for Zn-xSb solders were plotted as a function of indentation time, t, and presented in Fig. 4.13. It was observed that the H values of Zn-1.7wt% Sb were higher than that of other two alloys. As discussed in Microhardness, hardness was supposed to be increased in Zn-2.2wt% Sb, but it was decreased because of forming large IMC of Sb_3Zn_4 which weakened the structure and reduced the hardness. Moreover, this Figure 4.13 showed that

the H values for all solders indicated time dependence and they gradually decreased with increasing indentation time due to the indentation creep [65].

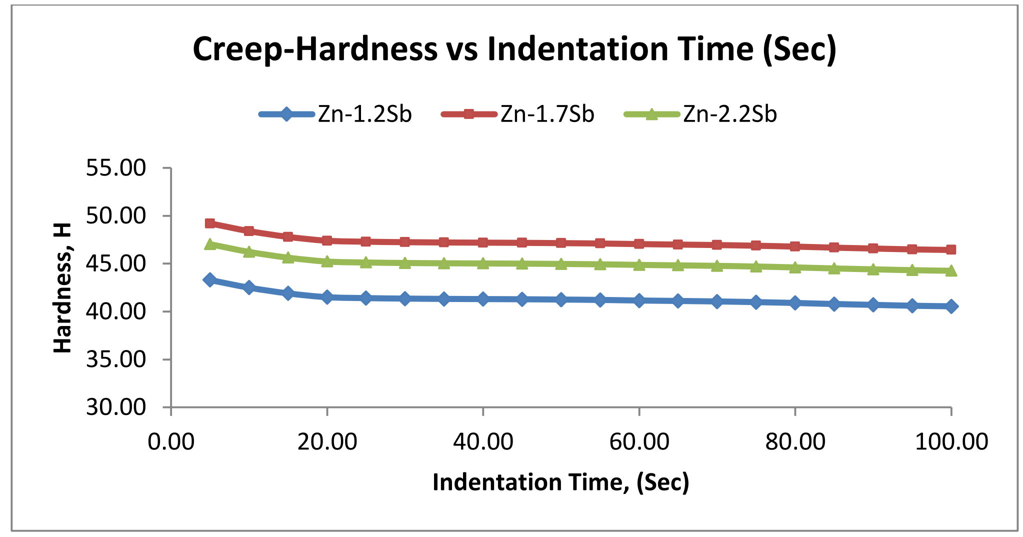

Figure 4. 13 Indentation time dependence of Hardness (H) for Zn-xSb-Creep behavior

As stated by Atkins, strain= $(1/H)^{1.5}$ and a plot of strain versus indentation time results in a creep curve that was similar to an ordinary creep curve [65]. The creep strain, during indentation process, was identified with $(1/H)^{1.5}$ and was therefore in arbitrary units.

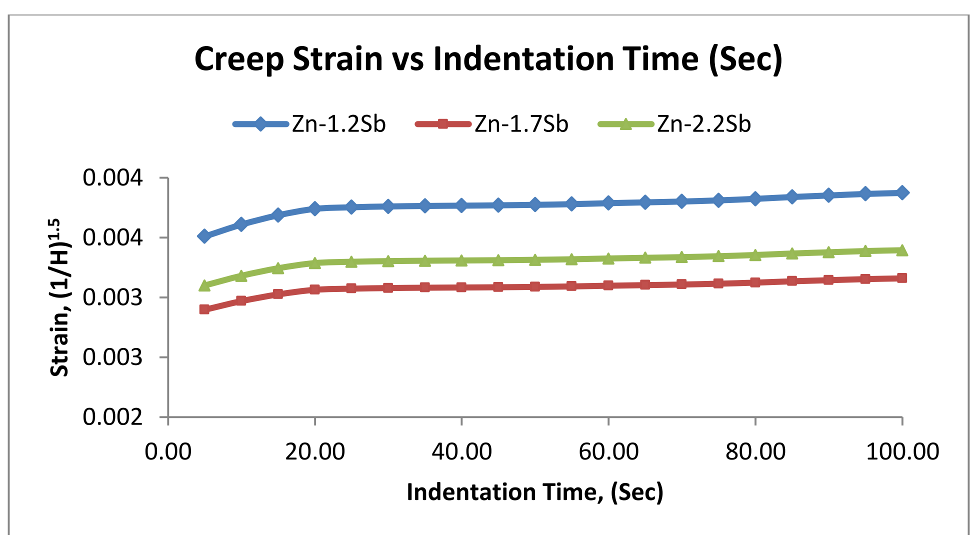

Figure 4. 14 Creep curves derived from Hardness (H) and Indentation time (t) for Zn-xSb [Appendix D]

Indentation creep curves derived from the hardness values are depicted in Fig. 4.14. The creep curves consist of two distinct stages; primary creep stage characterized by a decreasing creep rate followed by the secondary steady state creep stage characterized by a steady state creep rate. The secondary creep stage for the most Zn-xSb alloys seems to be attained after 20 sec. By using the hardness data, creep strain and indentation time chart was plotted and it was observed that the values of creep strain for Zn-1.7wt% Sb was lower than the same for other two alloys.

4.4 DISCUSSION ON OBSERVATIONS AND TEST RESULTS

To develop an appropriate Zn-based Pb-free solder alloy, various amount of Sb were added to the pure Zn and those were investigated for microstructural, mechanical, thermal and interfacial study for long-term soldering application.

The mechanical properties of solders were found to be highly dependent on their microstructure. It was found that the microstructure of the eutectic Zn-1.7wt% Sb studied in this research became refined because of lamellar structure and complete dissolution of Sb in Zn. As a result, the refined microstructure exhibited better mechanical properties, such as higher tensile strength and microhardness. The improvement in tensile strength has coincided with percent of elongation. Due to the refinement of microstructure of Zn-1.7wt% Sb solder alloy, it is reasonable to see a desired improvement in the microhardness for this binary alloy, even better than 63Sn-37Pb. The tensile strength and % of elongation for 1.7wt% Sb were also found optimum comparing with other two alloys. For higher amount of Sb (2.2wt%) addition in Zn-xSb eutectic solder alloy, tensile strength was found highest but unexpectedly brittle and very insignificant elongation. The sudden drop of tensile strength was believed for the non-coherent large precipitation of Zn_4Sb_3 intermetallic compound in the original interface results in a lower ductility. Elongation also falls due to the same reason of suitable slip plane movement restriction. Whatever, the optimum tensile properties found in eutectic alloy was still lower than that for 63Sn-37Pb. Electrical conductivity, the most important properties for solder alloys, was found higher in Zn-1.7wt% Sb, even it was found way better than 63Sn-37Pb.

To understand the melting behavior of the newly developed binary Pb-free solder alloys, DSC analysis was carried out. The melting temperature for eutectic Zn-1.7wt% Sb was found the lowest at 410.67°C comparing with other two alloys 416.50°C and 419.67 °C respectively. Thus, eutectic alloy ensured the expected lowest melting behavior. EDX and XRD were conducted to identify further crystallite phases in Pb-free Zn-xSb alloys. Both analysis confirmed the Zn and Zn_4Sb_3 phases in the alloys which obeyed the phase diagram and exhibited the microstructural and mechanical properties. To identify the creep strain behavior, microhardness data by using Vickers hardness tester was recorded for different indentation duration. It was found that hardness was higher for eutectic alloy whereas it was found lower in case of other two alloys of Zn-1.2wt% Sb and Zn-2.2wt% Sb. As creep strain is a function of hardness ($(1/H)^{1.5}$) and indentation time (t sec) duration, so it was found lowest for the eutectic Zn-1.7wt% Sb among these three solder alloys.

The above study showed that the Pb-free Zn-1.7wt% Sb eutectic solder could be suitable for practical applications to replace Sn-xPb alloy in line with environmental concern.

CHAPTER 5

AGEING

5.1 INTRODUCTION

Ageing of Metals- There are many alloys for which ageing is carried out as a special operation of heat treatment that ensures an aggregate of important mechanical and physical properties. **Ageing** or precipitation hardening is the principal method for the strengthening heat treatment of alloys. Artificial ageing is the treatment of a metal alloy at elevated temperatures so as to accelerate the changes in the properties of an alloy as a result of the casting and forging process. Generally, the chemical properties of newly cast and forged metals naturally change and settle very slowly at room temperature.

To observe the ageing effect in the microstructure and mechanical properties after heat treatment, Ageing was done at same temperature for different time duration. Since the eutectic Zn-1.7wt% Sb had the most optimum properties for being an appropriate solder alloy, so two samples of eutectic alloy were taken to be aged in an automatic digital induction furnace for two different time duration namely 250 hours and 500 hours at 200 °C. Then samples were taken out from the furnace and let those be cooled down in air to room temperature. Later, those were investigated for the ageing effect in microstructure and mechanical properties.

5.2 MICROSTRUCTURAL ANALYSIS

5.2.1 Microstructure under OM and SEM

Cubic samples were prepared with same dimensions of 10mm x 10mm x 10mm like as-cast samples described in previous chapters and investigated the sample by optical microscope (OM) and micrographs were recorded with a digital camera and followed by scanning electron microscope (SEM) . Also, energy dispersive x-ray (EDX) analysis was used to determine the elemental compositions at selected spots and areas. The backscattered electron imaging mode of the SEM was used to study the microstructure.

In the sample aged for 250 hours, the particles got enough time to precipitate results the increased amount of precipitation over the time. This adequate precipitation expedited the formation of medium sized particles precipitated in Zn matrix which is shown in Fig-5.1 c & d. On the other hand, ageing done for 500 hours facilitated unnecessarily excess time for the precipitation and let the particles to grow and become coarser. This phenomenon is recognized as over-ageing. Coarse precipitated particles due to over-ageing for 500 hours are given Fig-5.1 e and f.

Figure 5. 1 Optical micrographs of the chill-cast samples of Zn-1.7wt% Sb non-aged in (a) and (b) at 200X and 500X respectively, Zn-1.7wt% Sb aged for 250 hours in (c) & (d) at 200X and 500X respectively, Zn-1.7wt% Sb aged for 500 hours in (e) & (f) at 200X and 500X respectively

The microstructures of samples were also examined under scanning electron microscope (SEM) in Secondary Electron Imaging (SEI) mode shown in Figure 5.2 a-c.

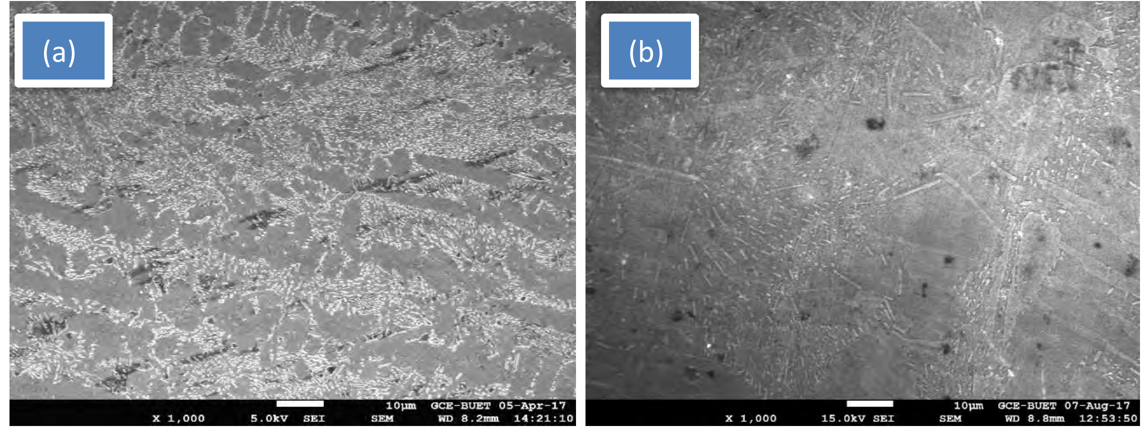

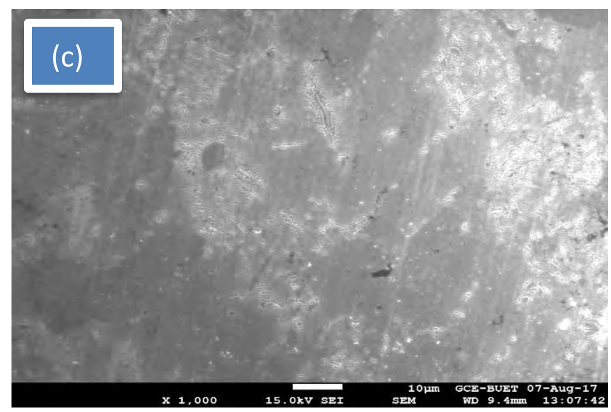

Figure 5. 2 SEM microstructure in SE mode of chill-cast samples of (a) Zn-1.7wt% Sb, (b) Zn-1.7wt% Sb aged for 250 hours, and (c) Zn-1.7wt% Sb aged for 500 hours (all images taken at 1000 X).

Figure 5.2 a has presented the finer microstructure of as-cast eutectic alloy whereas Fig 5.2 b has shown the microstructure with more precipitated particles of the alloy aged for 250 hours. Fig 5.2 c has exhibited the microstructure with coarser particles formed due to over-aged for 500 hours.

5.2.2 Energy Dispersive X-ray (EDX) Analysis

Like as described in previous chapter, EDX analysis was used in order to analyze the distribution of different elements in different phases, to determine the elemental composition at selected areas and spots.

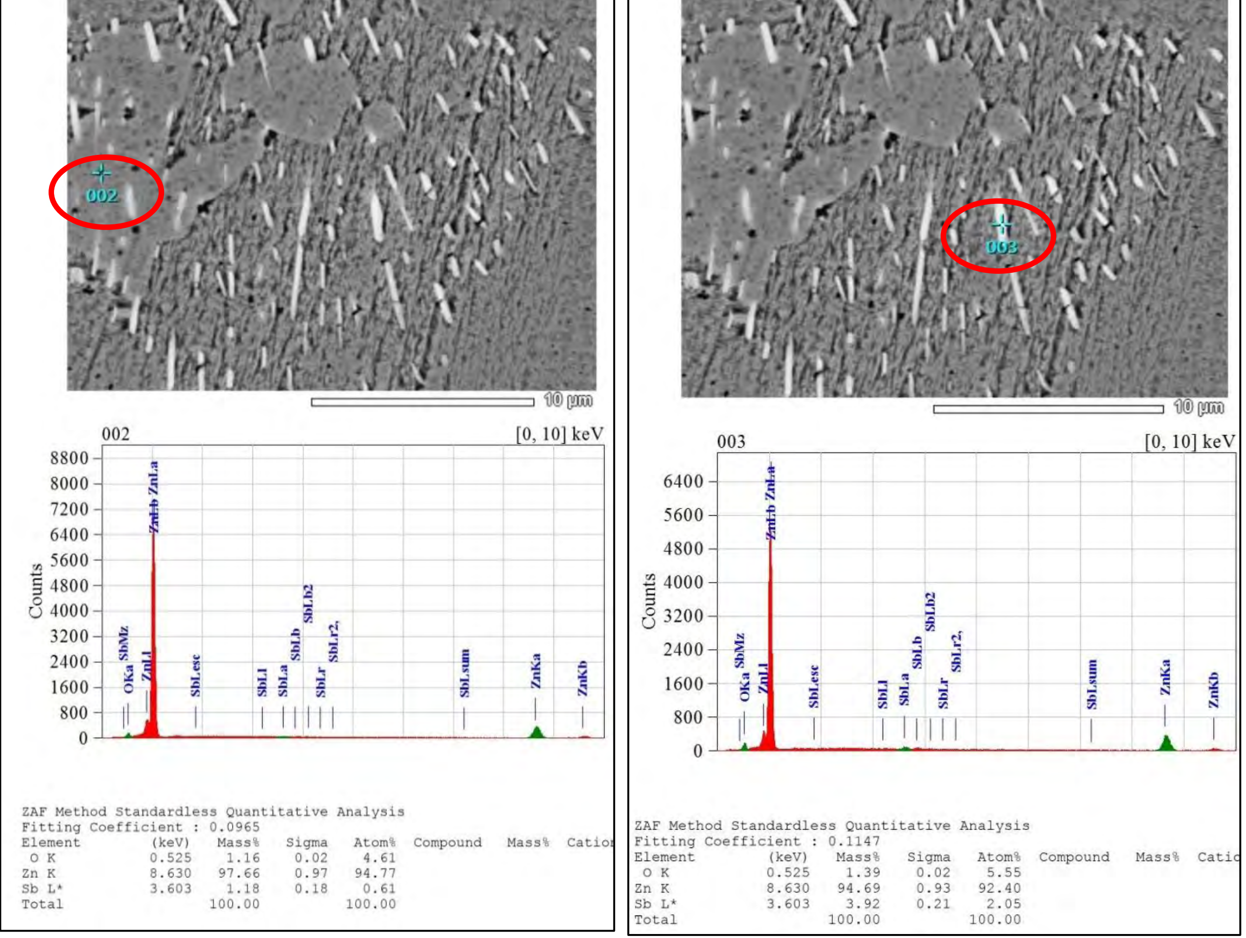

Figure 5. 3 SEM microstructure of chill-cast Zn-1.7wt% Sb aged 250 hours with EDX spectrum

First point in Fig 5.3 exhibited the complete eutectic mixture with composition of approximately 98wt% Zn and 1.2%wt Sb whereas second point in Fig 5.3 showed the composition of the whitish rod like phase pointed with round circle containing the Sb-rich ε-Sb_3Zn_4 phase.

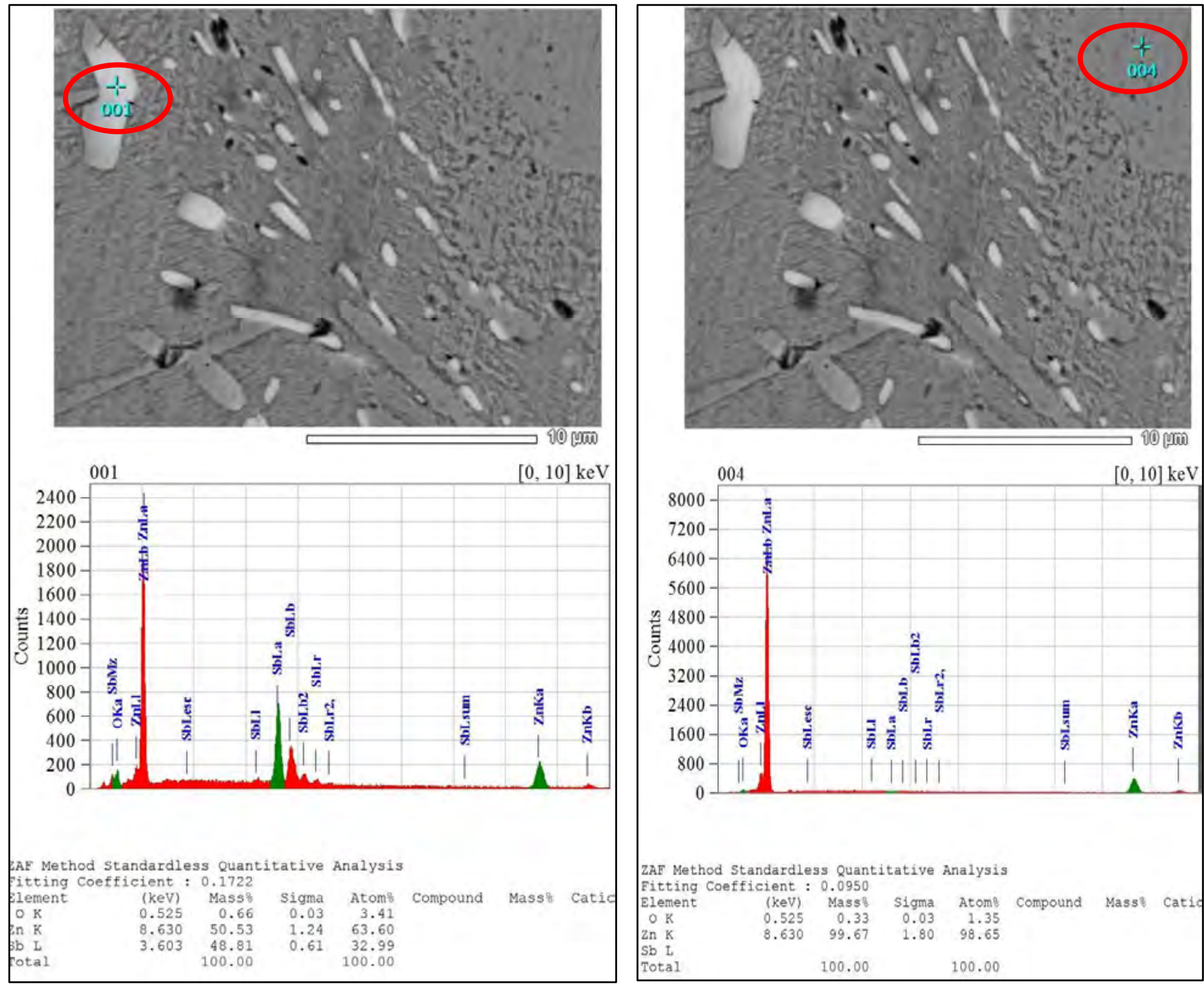

Figure 5. 4 SEM microstructure of chill-cast Zn-1.7wt% Sb aged 500 hours with EDX spectrum

Fig 5.4 has clearly revealed the coarse whitish bigger particles with the composition of 50wt% Zn and rest wt% Sb on the gray colored Zn matrix.

5.3 ANALYSIS ON MECHANICAL PROPERTIES

5.3.1 Melting Behavior Analysis

The differential scanning calorimeter (DSC) analysis was also used to determine the melting and solidification characteristics of the samples. Comparing the Figure 5.5 a, b & c, an insignificant change in melting temperature was found after ageing. Samples having aged for 250 hours and 500 hours got the melting temperature at 411.48 ºC and 412.76 ºC respectively. So it indicates that the ageing done for different time duration at same temperature does not cause of significant change in melting behavior.

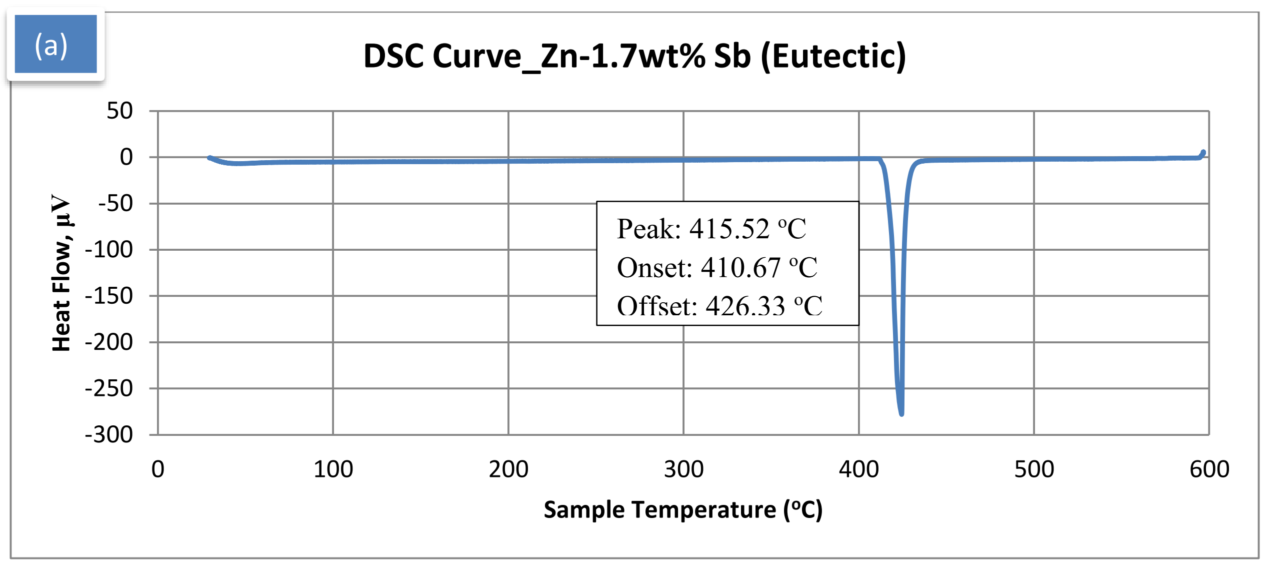

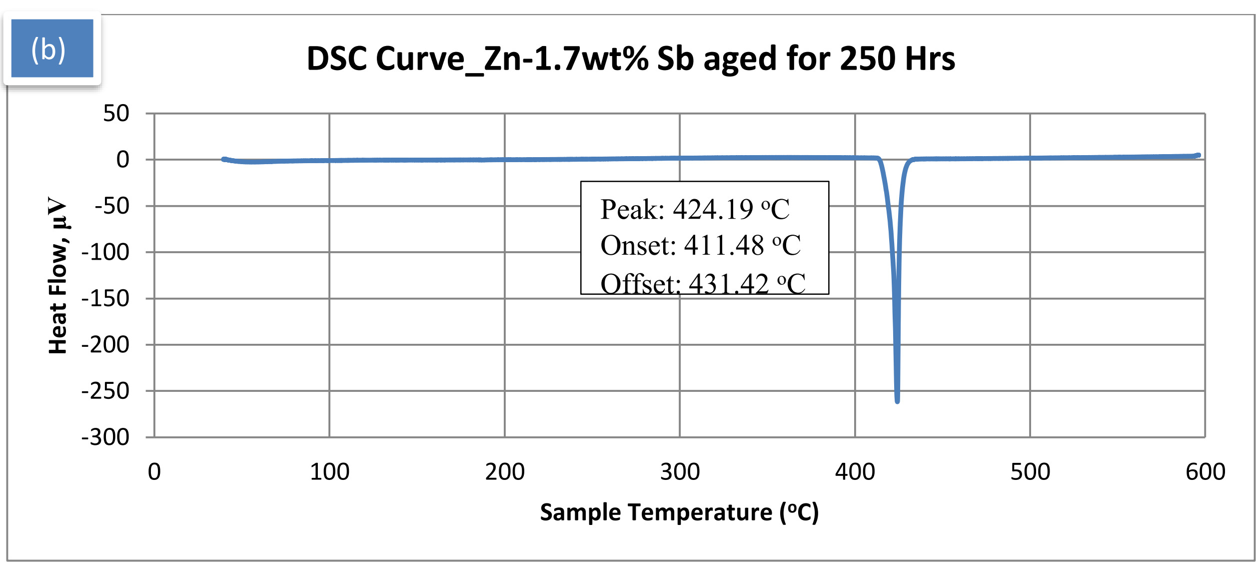

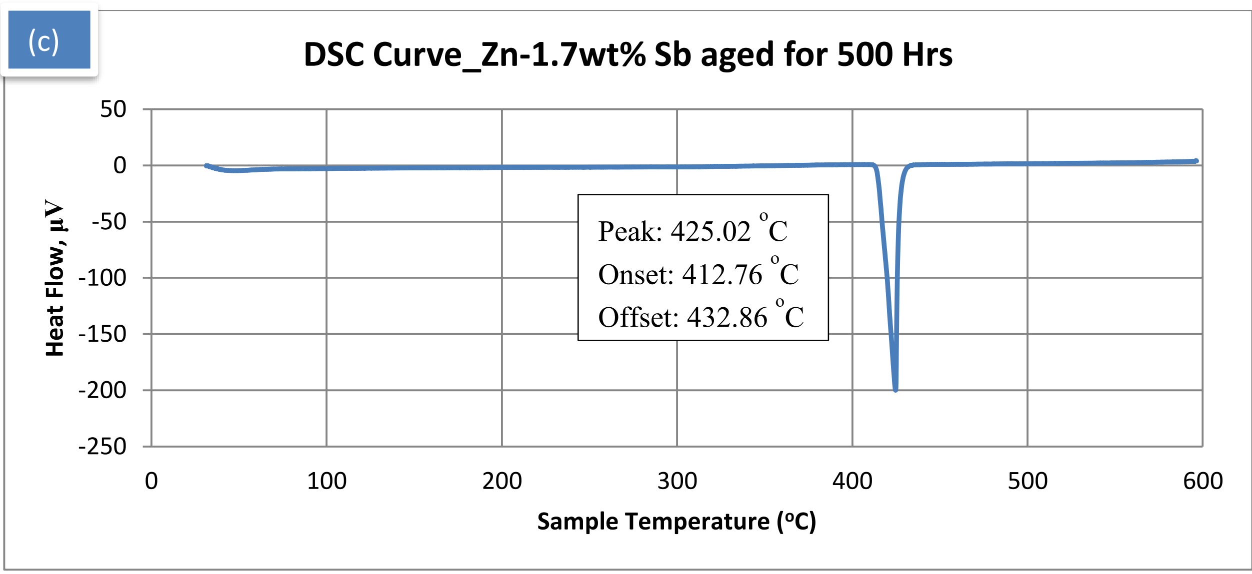

Figure 5. 5 The DSC curves on heating of (a) eutectic Zn -1.7wt% Sb, (b) Zn-1.7wt% Sb aged 250 hours at 200°C, (c) Zn-1.7wt% Sb aged 500 hours at 200°C [Appendix A]

5.3.2 Microhardness Test

Usually Ageing facilitates to remove the foreign materials and let the lattice particles grow further resulting the higher strength in alloy, but excessive ageing time usually leads to over-ageing by precipitate coarsening resulting in loss of strength. [Appendix B]

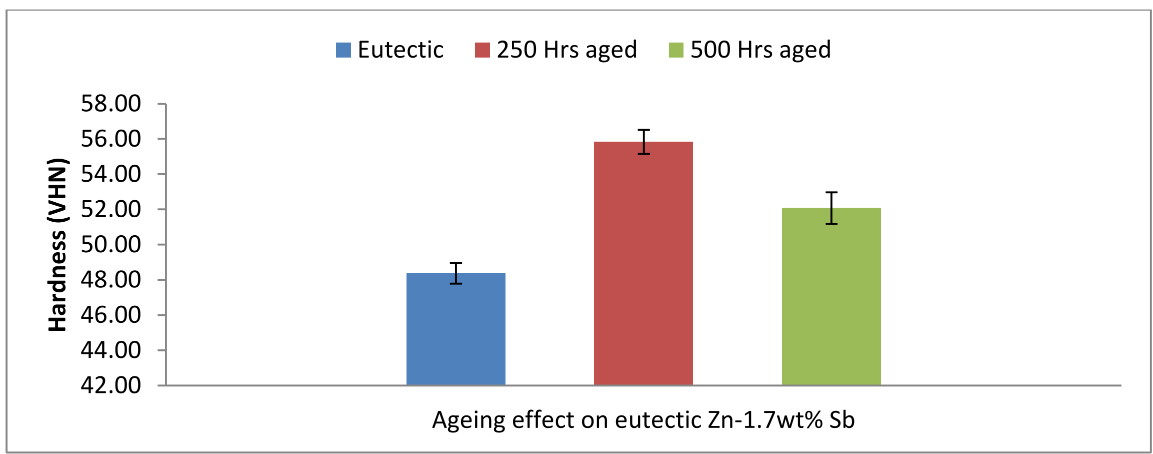

Figure 5. 6 Ageing effect on microhardness of eutectic alloy

It is observed from the Figure 5.6 that the hardness was found higher for the sample aged for 250 hours than that for non-aged Zn-1.7wt% Sb alloy. Again it was decreased slightly in the sample over aged for 500 hours, because of very fast hardening due to the rapid diffusion. So optimum hardening (55.84) was ensured in the sample aged within reasonable length of time-250 hours which was also higher than the hardness number (12.20) of 63Sn-37Pb alloy as mentioned in previous chapter as well.

5.3.3 Tensile Test

Tensile strength was observed higher in the sample aged for 250 hours than other two alloys as because of the precipitation hardening during ageing. But UTS was found lower in case of ageing for 500 hours because of the over-ageing which caused the reduction of strength shown in Fig 5.7. Tensile properties were found higher in 250 hours aged samples than 63Sn-37Pb which was previously lower in un-aged samples.

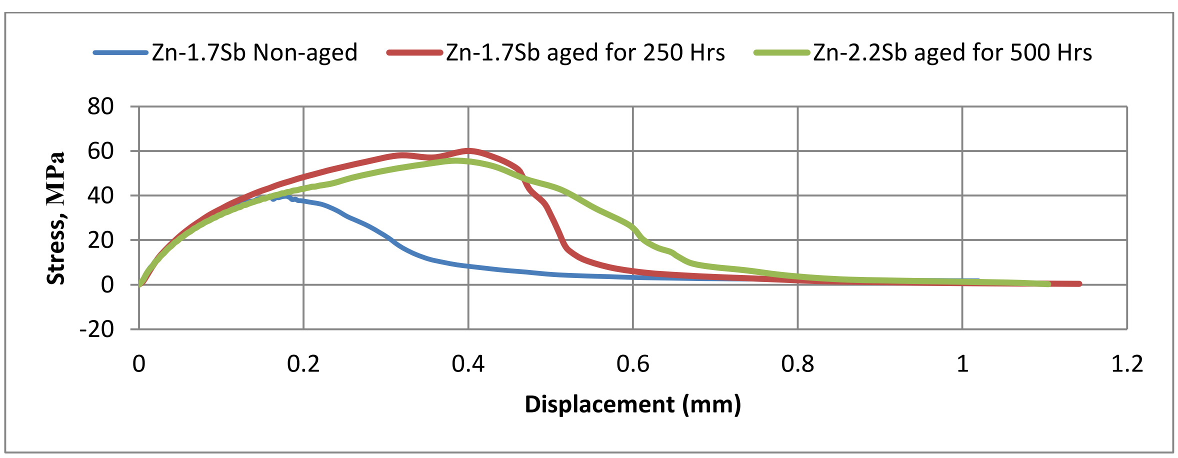

Figure 5. 7 Tensile strength after ageing [Appendix C]

Table 5. 1 Mechanical properties of Zn-1.7wt% Sb non-aged, aged for 250 hours and aged for 500 hours [Appendix C]

Alloys	Melting point, (ºC)	Micro hardness, (VHN)	Tensile Strength, (MPa)	Elongation, (%)
Eutectic non-aged	410.12	48.38	40	38
Eutectic aged for 250 hours	411.48	55.84	60	65
Eutectic aged for 500 hours	412.76	52.08	56	58

5.3.4 Electrical Conductivity Analysis

The measurement of electrical conductivity is an indirect way to understand the nature and distribution of the precipitates in the part as the conductivity is highly sensitive to the chemical composition of the alloy.

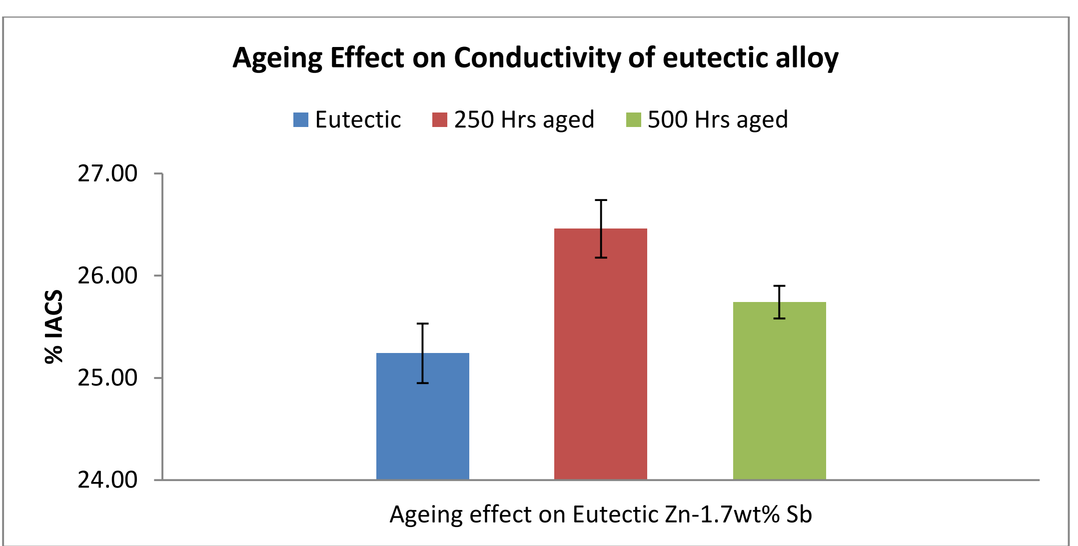

Figure 5. 8 Ageing effect on electrical conductivity

The removal of foreign atoms from the parent lattice during precipitation hardening removed much of the distortion of the electron distribution in the lattice. This action favored the movement of electrons through the metal and resulted in higher conductivity in the sample aged for 250 hours. But rapid diffusion during over-ageing in third sample (aged for 500 hours) led to the coarsening precipitation and distorted the particle orientation resulted the lower conductivity. So highest conductivity (26.46) was observed for the sample aged for 250 hours presented in Fig 5.8, even much higher than 63Sn-37Pb.

5.3.5 X-ray Diffraction (XRD) Analysis

The peaks pattern presented in Fig 5.9 showed the similarity with the patterns found for the eutectic non aged alloy. However, higher intensity in the prominent peak at 37° was occurred for the sample aged for 500 hours, on the other hand the same was found at 43° for non-aged eutectic alloy than other two alloys. Eventually, XRD analysis verified the phases in the alloys found in the eutectic as cast alloy.

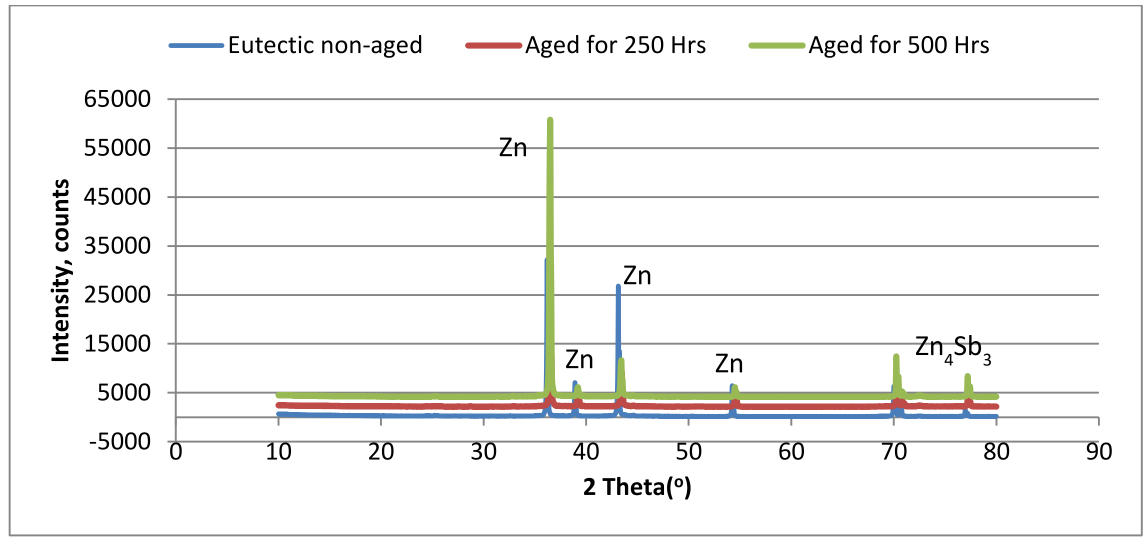

Figure 5. 9 X-Ray diffraction patterns of non-aged and aged eutectic alloys

5.3.6 Creep Behavior Analysis

The results obtained for the hardness, H, for non-aged and aged Zn-1.7wt% Sb solders were plotted as a function of indentation time, t, and presented in Fig. 5.10. As discussed in the Microhardness section, the higher H values were observed for the alloy aged for 250 hours than the as-cast sample. On the other hand, hardness exhibited an anomalous behavior for Zn-1.7wt% Sb aged for 500 hours due to the coarsening effect described in previous sections.

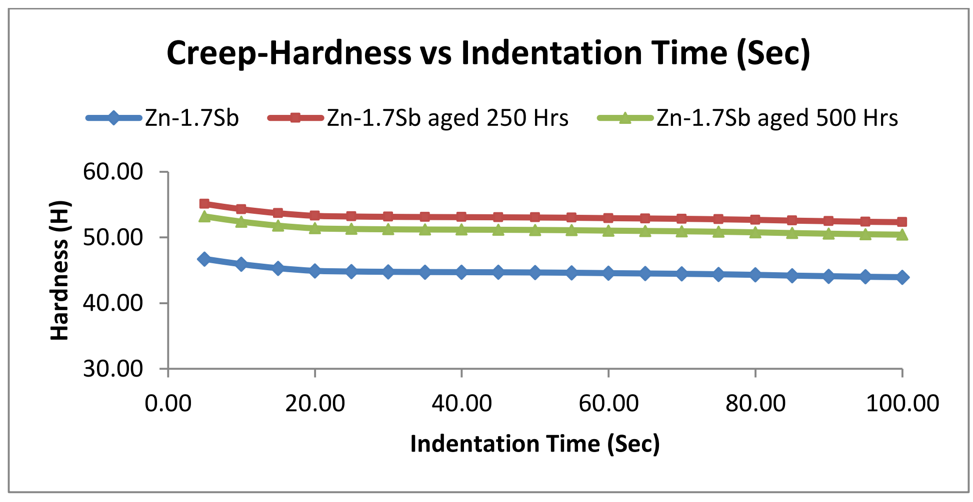

Figure 5. 10 Indentation time dependence of Hardness (H) for Zn-xSb aged for 250 hours and 500 hours-Creep behaviors

In Fig 5.10, Creep hardness (H) values have been plotted against the indentation times (t) [65]. As the hardness for the sample aged for 250 hours is much higher than other two alloys, so consequentially creep strain $(1/H)^{1.5}$ was found lower shown in Fig 5.11.

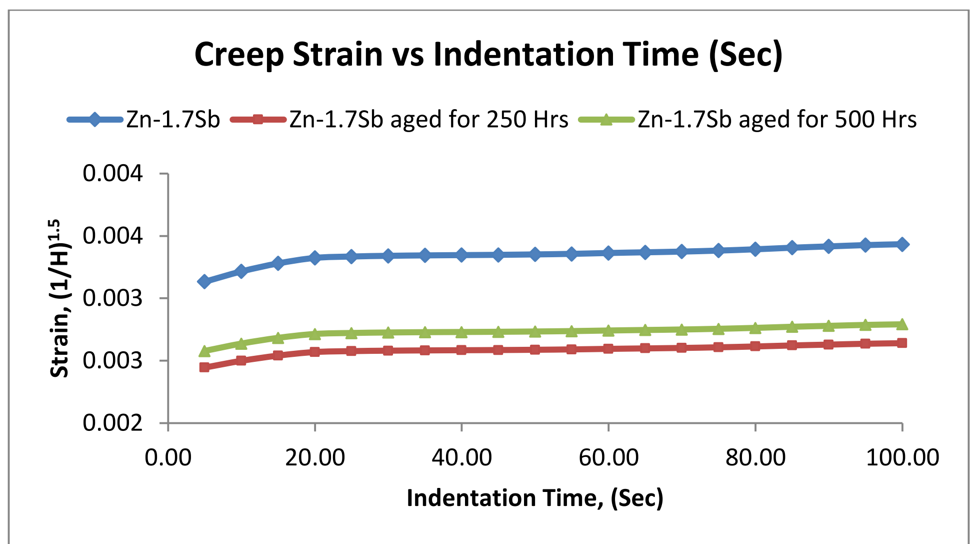

Figure 5. 11 Creep curves derived from Hardness (H) and Indentation time for Zn-1.7wt% Sb aged for 250 hours and 500 hours [Appendix D]

CHAPTER 6

CONCLUSION

Since most widely used Pb-based solder alloy has become an environmental issue and the rising awareness on pollution strictly encourages in replacing it. So the aim of this study was to develop an appropriate alternative solder alloy and thus three different compositions of Zn-xSb were selected including the eutectic alloy. The newly developed binary solders were investigated for microstructural, mechanical, thermal and interfacial study and identified those with competitive performances than the Pb-based solders specifically 63Sn- 37Pb.

As mentioned in the discussion part in previous chapter, microstructure influences and fixes the mechanical properties of the solders. Since higher precipitation hardening was observed in the microstructure of the eutectic alloy aged for 250 hours, so it led to the better mechanical properties, especially it improved tensile strength to make it better than 63Sn-37Pb which was lower in un-aged eutectic alloy. These characteristics can clearly be explained by the dispersion strengthening theory; i.e. the particles got enough time during ageing to precipitate in the matrix results an increase in tensile strength, the term also called precipitation strengthening. The tensile strength fallen down in 500 hours aged sample due to the over-ageing is believed for the non-coherent large precipitation Zn_4Sb_3 intermetallic compound. The non-coherency of big IMCs in turn weakened the original matrix interface with those large IMCs, resulted a lower tensile strength.

In DSC analysis, there was no significant difference in melting temperature due to the ageing. EDX analysis was carried out to identify the components in line with the respective stoichiometry. On the other hand, XRD analysis was also conducted to cross match with the EDX and to identify the three major phases of Zn and Zn_4Sb_3 intermetallic compound. Peak patterns of these phases matched with the individual original peaks.

Creep behavior was also identified by using the Vickers microhardness at different indentation duration. It was observed that hardness decreased with the increasing of indentation time. As creep strain has an inverse relation ($(1/H)^{1.5}$) with hardness, so it was found increasing as decreasing the hardness. Lower creep strain was resulted in the 250 hours aged sample due to having higher hardness.

Therefore, the eutectic alloy Zn-1.7wt% Sb aged for 250 hours at 200 °C had the desired microstructural properties as well as higher hardness, tensile strength and electrical conductivity comparing to the mostly used 63Sn-37Pb solder alloy which can be the properties of the most competitive high temperature solder alloy in replacing the Pb-based solders for long run soldering application.

REFERENCES:

1. Carlin, C. M., & Ray, J. K. (1994, June). The Requirements for High Temperature Electronics in a Future High Speed Civil Transport (HSCT). In Proc. 2nd Int. High Temperature Electronics Conf (pp. 19-26).
2. Brown, R. B., Terry, F. L., Wu, K., & Krischman, R. K. (1999). High-Temperature E.
3. Vermesan, O., Riisnæs, K. H., Le Pailleur, L., Nysæther, J. B., Bauge, M., Rustad, H. & Pezzani, R. (2003). A 500-dpi AC capacitive hybrid flip-chip CMOS ASIC/sensor module for fingerprint, navigation, and pointer detection with on-chip data processing. Solid-State Circuits, IEEE Journal of, 38(12), 2288-2296.
4. Neudeck, P. G., Okojie, R. S., & Chen, L. Y. (2002). High-temperature electronics-a role for wide bandgap semiconductors?. Proceedings of the IEEE, 90(6), 1065-1076.
5. Namhyun Kang a, Hye Sung Na a, Seong Jun Kim b, Chung Yun Kang "Alloy design of Zn–Al–Cu solder for ultra-high temperatures" Journal of Alloys and Compounds 467 (2009) 246–250
6. Islam, M. N., Sharif, A., & Chan, Y. C. (2005). Effect of volume in interfacial reaction between eutectic Sn-3.5% Ag-0.5% Cu solder and Cu metallization in microelectronic packaging. Journal of electronic materials, 34(2), 143-149.
7. Tsai, J. Y., Chang, C. W., Shieh, Y. C., Hu, Y. C., & Kao, C. R. (2005). Controlling the microstructure from the gold-tin reaction. Journal of electronic materials, 34(2), 182-187.
8. Song, H. G., Ahn, J. P., & Morris, J. W. (2001). The microstructure of eutectic Au-Sn solder bumps on Cu/electroless Ni/Au. Journal of electronic materials, 30(9), 1083-1087.
9. Song, J. M., Chuang, H. Y., & Wu, Z. M. (2006). Interfacial reactions between Bi-Ag high-temperature solders and metallic substrates. Journal of electronic materials, 35(5), 1041-1049.
10. Lalena, J. N., Dean, N. F., & Weiser, M. W. (2002). Experimental investigation of Ge-doped Bi-11Ag as a new Pb-free solder alloy for power die attachment. Journal of electronic materials, 31(11), 1244-1249.
11. Suganuma, K., Kim, S., 2010. Ultra heat-shock resistant die attachment for silicon carbide with pure zinc. Electron Device Letters, IEEE 31 (12), 1467–1469.
12. Park, S.W., Sugahara, T., Kim, K.S., Suganuma, K., 2012. Enhanced ductility and oxidation resistance of Zn through the addition of minor elements for use in wide-gap semiconductor die-bonding materials. Journal of Alloys and Compounds 542, 236–240. J. Yu, D.K. Joo, S.W. Shin, Acta Matter 50 (2002) 4315.
13. Kim, S. J., Kim, K. S., Kim, S. S., Kang, C. Y., &Suganuma, K. (2008). Characteristics of Zn-Al-Cu alloys for high temperature solder application. Materials transactions, 49(7), 1531-1536.
14. Shimizu, T., Ishikawa, H., Ohnuma, I., & Ishida, K. (1999). Zn-Al-Mg-Ga alloys as Pb-free solder for die-attaching use. Journal of electronic materials, 28(11), 1172-1175
15. Rosilli, R., Ariff, A. H. M., &Zam, S. F. M. (2014). Bi-Ag as an Alternative High Temperature Solder. Pertanika Journal of Science & Technology, 22(1), 1-13.
16. J. S. Hwang, "Modern Solder Technology for Competitive Electronics Manufacturing", New York: McGraw-Hill, (1996).
17. E. R. Monsalve, "Lead ingestion hazard in hand soldering environments", Proceedings of the 8th Annual Soldering Technology and Product Assurance Seminar, February (1984), Naval Weapons Center, China Lake, CA.

18. D. Napp, “Lead-free interconnect materials for the electronics industry”, Proceedings of the 27th International SAMPE Technical Conference, Albuquerque, NM, 9–12 October (1995), p.342.
19. E. P. Wood, and K. L. Nimmo, “In Search of New Lead-free Electronic Solders”, J. Electron. Mater. **23**(8), (1994), pp.709-714.
20. K. Gerahty, “An update of WEEE and RoHS directives”, Circuit World, **29**(4), (2003).
21. “ASM International, Electronic Material Handbook 1”, Materials Park, OH, (1989).
22. Manifa Noor and Ahmed Sharif, “Bi Based Interconnect Systems and Applications” in Chapter 9.
23. Kim, J. H., Jeong, S. W., & Lee, H. M. (2002). Thermodynamics-aided alloy design and evaluation of Pb-free solders for high-temperature applications. Materials transactions, 43(8), 1873-1878.
24. Spinelli, J. E., Silva, B. L., Cheung, N., & Garcia, A. (2014). The use of a directional solidification technique to investigate the interrelationship of thermal parameters, microstructure and microhardness of Bi–Ag solder alloys. Materials Characterization, 96, 115-125.
25. Massalski, T. B. (1992). Binary Alloy Phase Diagrams. ASM International, Metals Park, OH.
26. Villars, P., Cenzual, K., Daams, J. L.C., Hulliger, F., Massalski, T.B., Okamoto, H., Osaki,K.,Prince, A., & Iwata, S. (2003). Inorganic Materials Database and Design System, Crystal Impact, Pauling File. Binaries Edition, AS International, Metal Park, OH.
27. Chidambaram, V., J. Hattel, and J. Hald, *High-temperature lead-free solder alternatives.* Microelectronic Engineering, 2011. **88**(6): p. 981-989.
28. Ayesha akter1, Hasan M. Usama1 and Rubayyat Mahbub, “Gold Based Interconnect Systems for High Temperature and Harsh Environment”
29. Mallick, S., Kabir, M. and Sharif, A. (2016). Study on the properties of Zn–xNi high temperature solder alloys. Journal of Materials Science: Materials in Electronics, 27 (4), 3608-3618.
30. F. O. P. Vollweier, Intermetallic grow that the interface between copper and bismuth-tin solder, Thesis of Master of Science, Naval Postgraduate School, Monterey, California, 1993.
31. W. L. Winterbottom, Converting to lead-free solders: an automobile industry perspective, Journal of Minerals, Metals & Materials Society, 45, 1993, pp.20-26.
32. Md Khairul Islam, Ahmed Sharif, 2016, “Characterization of Zn-xMo alloy for high temperature soldering application” Proceedings of the International Conference on Mechanical Engineering 2016 (ICME2016) 22- 24 December 2016, Dhaka, Bangladesh, pp. 01-06.
33. Thesis work of Md Khairul Islam on “Characterization of Zinc based high temperature solder alloys with Chromium and Molybdenum additions” in February 2017
34. T. Nagaoka, Y. Morisada, M. Fukusumi and T. Takemoto, Selection of soldering temperature for ultrasonic-assisted soldering of 5056 Al alloy using Zn–Al system solders, Journal of Materials Processing Technology, 211, 2011, pp. 1534–1539.
35. J. Moses, The Practicing Scientist’s Handbook, Van Nostrand Reinhold, New York, 1978.
36. J. A. Wasynczuk and G.K. Lucey, Shearcreep of Cu_6Sn_5eutectic composites, Proceedings of the Technical Program, National Electronic Packaging and Production Conference, Nepcon West, vol. 3, Des Plains, IL, 1992, pp. 1245– 1255.

37. K. Suganuma, S. J. Kim and K. S. Kim, High temperature lead-free solders: properties and possibilities, Journal of Minerals, Metals and Materials, 64, 2009, pp. 64–71.
38. S. M. L. Sastry, T.C. Peng, R.J. Lederich, K.L. Jerina and C.G. Kuo, Microstructures and mechanical properties of in-situ composite solders, Proceedings of Technical Program—Nepcon West Conference, Anahein, CA, 1992, Cahners Exhibition Group, Des Plains, IL, 3, 1992, p. 1266.
39. J. A. Wasynczuk and G. K. Lucey, Shearcreep of Cu_6Sn_5eutectic composites, Proceedings of the Technical Program, National Electronic Packaging and Production Conference, Nepcon West, vol. 3, Des Plains, IL, 1992, pp. 1245– 1255.
40. T. Takahashi, S. Komatsu, H. Nishikawa and T. Takemoto, Improvement of high-temperature performance of Zn-Sn solder joint, Journal of Electronic Materials, 39, 2010, pp. 1241-1247.
41. Namhyun Kang a, Hye Sung Na a, Seong Jun Kim b, Chung Yun Kang "Alloy design of Zn–Al–Cu solder for ultra-high temperatures" Journal of Alloys and Compounds 467 (2009) 246–250
42. S. J. Kim, K. S. Kim, S. S. Kim, C. Y. Kang and K. Suganuma, Characteristics of Zn-Al-Cu alloys for high temperature solder application, Materials Transactions, 49, 2008, pp. 1531-1536.
43. A. Sharif, "A Study on Interfacial Interaction Behavior Between Lead-Free Solders and Electroless Nickel Metallization for Advanced Electronic Packaging", Ph. D. Thesis, City University of Hong Kong, Hong Kong, (2005)
44. J. A. Wasynczuk and G.K. Lucey, Shearcreep of Cu_6Sn_5eutectic composites, Proceedings of the Technical Program, National Electronic Packaging and Production Conference, Nepcon West, vol. 3, Des Plains, IL, 1992, pp. 1245– 1255.
45. Mallick, S., Kabir, M. and Sharif, A. (2016). Study on the properties of Zn–xNi high temperature solder alloys. Journal of Materials Science: Materials in Electronics, 27 (4), 3608-3618.
46. Kang, N., Na, H. S., Kim, S. J., & Kang, C. Y. (2009). Alloy design of Zn–Al–Cu solder for ultra high temperatures. Journal of alloys and compounds, 467(1), 246-250.
47. Shimizu, T., Ishikawa, H., Ohnuma, I., & Ishida, K. (1999). Zn-Al-Mg-Ga alloys as Pb-free solder for die-attaching use. Journal of electronic materials, 28(11), 1172-1175.
48. Cheng, F., Gao, F., Wang, Y., Wu, Y., Ma, Z., Yang, J. (2012). Sn addition on the tensile properties of high temperature Zn−4Al−3Mg solder alloys. Microelectronics Reliability 52 (3), 579–584.
49. Islam, M.K., Sharif, A. (2016). Zn-Based Solders for High Temperature Electronic Application. In: Saleem Hashmi (Editor-in-chief), Reference Module in Materials Science and Materials Engineering. Oxford: Elsevier; pp. 1-10.
50. Bae, Jee-Hwan, Keesam Shin, Joon-Hwan Lee, Mi-Yang Kim, and Cheol-Woong Yang. "Development of High-Temperature Solders: Contribution of Transmission Electron Microscopy." Applied Microscopy 45, no. 2 (2015): 89-94.
51. Zeng, G., Mcdonald, S., & Nogita, K. (2012). Development of high-temperature solders: Review. Microelectronics Reliability, 52(7), 1306-1322.
52. S. W. Chen, C. C. Lin and C. M. Chen, "Determination of the Melting and Solidification Characteristics of Solders Using Differential Scanning Calorimetry", Metall. Mater. Trans. A, **29**, (1998), pp.1965-1972.
53. Terry Dishongh, Cemal Basaran, Alexander N. Cartwright, Member, IEEE, Ying Zhao, and Heng Liu "Impact of Temperature Cycle Profile on Fatigue Life of Solder Joints" in IEEE Transactions on Advanced Packaging VOL. 25, NO. 3, AUGUST 20

54. Manual, DSC Q-10 Differential Scanning Calorimeter.
55. D. Frear, H. Morgan, S. Burchett and J. Lau, "The Mechanics of Solder Alloy Interconnects", New York: Van Nostrand Reinhold, (1994).
56. Mansur Ahmed, Tama Fouzder, A. Sharif, Asit Kumar Gain, Y.C. Chan, "Influence of Ag micro-particle additions on the microstructure, hardness and tensile properties of Sn–9Zn binary eutectic solder alloy", Volume 50, Issue 8, August 2010, Pages 1134-1141
57. Islam, M.N., Sharif, A. & Chan, Y.C. "Effect of Volume in Interfacial Reaction between Eutectic Sn-3.5% Ag-0.5% Cu Solder and Cu Metallization in Microelectronic Packaging", February 2005, Volume 34, Issue 2, pp 143–149
58. K. Mohan Kumar, V. Kripesh, Andrew A. O. Tay "Influence single-wall carbon nanotube addition on the microstructural and tensile properties of Sn-Pb solder alloy", January 2016, Journal of Alloys and Compounds, Volume 455, pp 148-158
59. Website: http://www.gordonengland.co.uk/hardness/hvconv.htm
60. W. D. Callister, "Materials Science and Engineering an Introduction", Canada: John Wiley & Sons Inc. 4th Edition, (1996).
61. https://www.nde-ed.org/EducationResources/CommunityCollege/Materials/Physical_Chemical/Electrical.htm, access date November 19, 2017
62. Islam MK, Sharif A., (2017), Characterization of zinc based high temperature solder alloys with chromium and molybdenum additions, MSc thesis, BUET, Dhaka-1000, pp-68
63. Website: https://en.wikipedia.org/wiki/Zinc and https://en.wikipedia.org/wiki/Antimony
64. Website: http://alasir.com/reference/solder_alloys/
65. F. Abd El-Rehim, H. Y. Zahran, S. AlFaify "The mechanical and microstructural changes of Sn-Ag-Bi solders with cooling rate and Bi content variations" Journal of Materials Engineering and Performance, Mnauscript ID JMEP-17-05-13041

APPENDIX

APPENDIX A

(a) Zn-1.2wt% Sb:

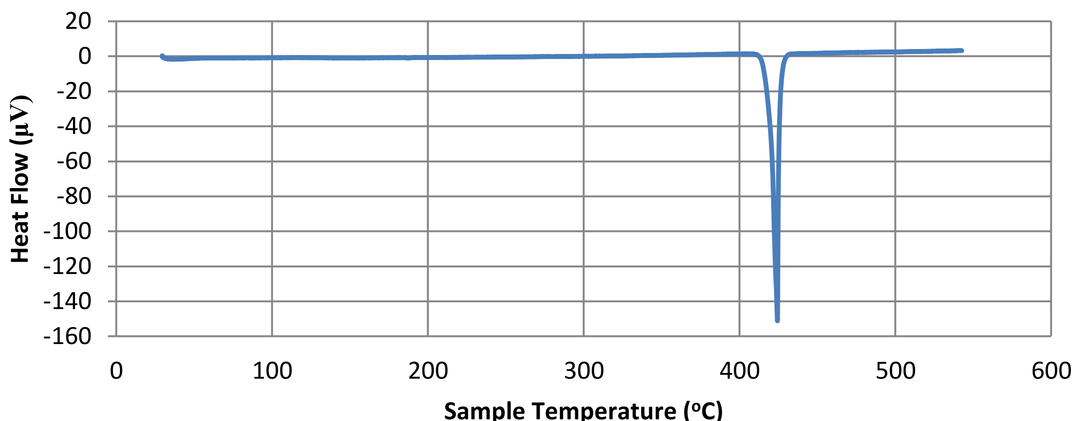

(b) Zn-1.7wt% Sb(Eutectic):

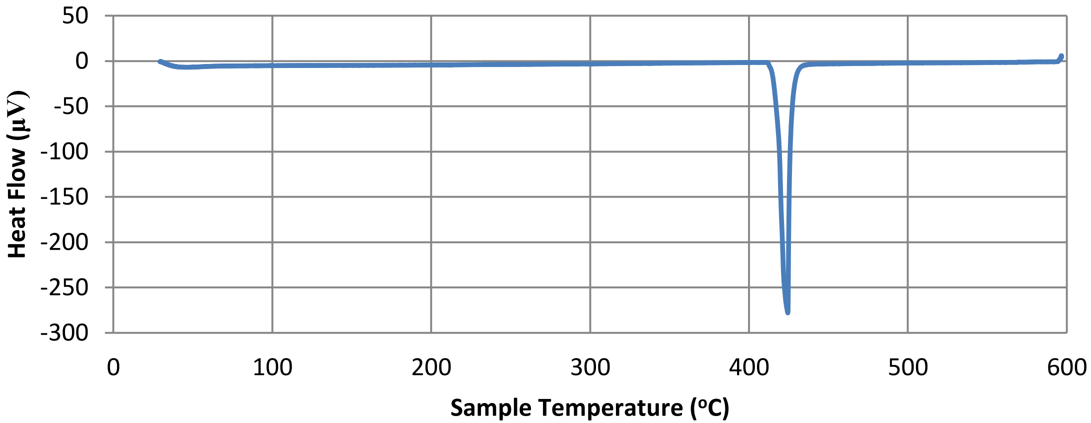

(c) Zn-2.2wt% Sb:

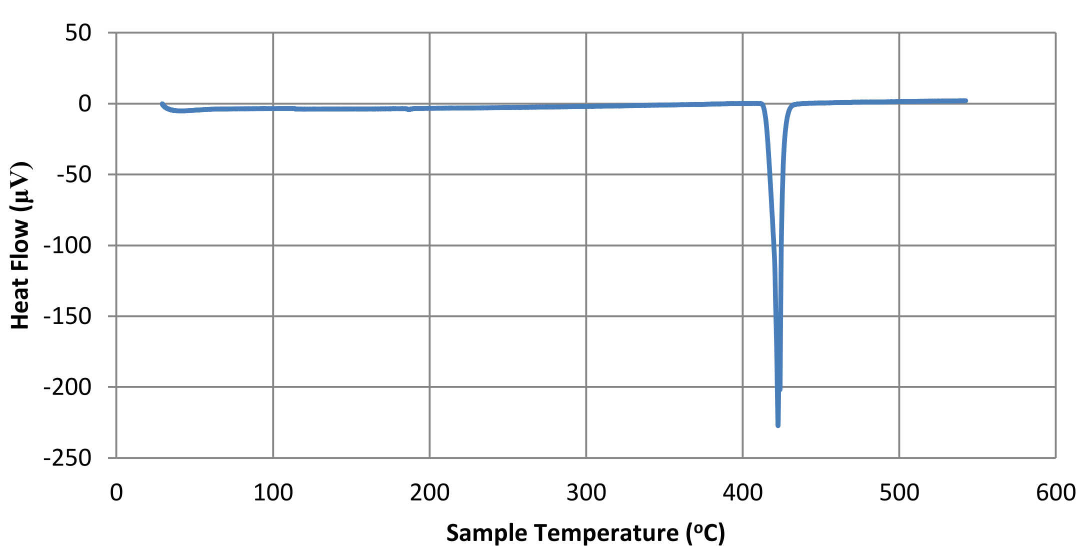

(d) Zn-1.7wt% Sb aged for 250 hours:

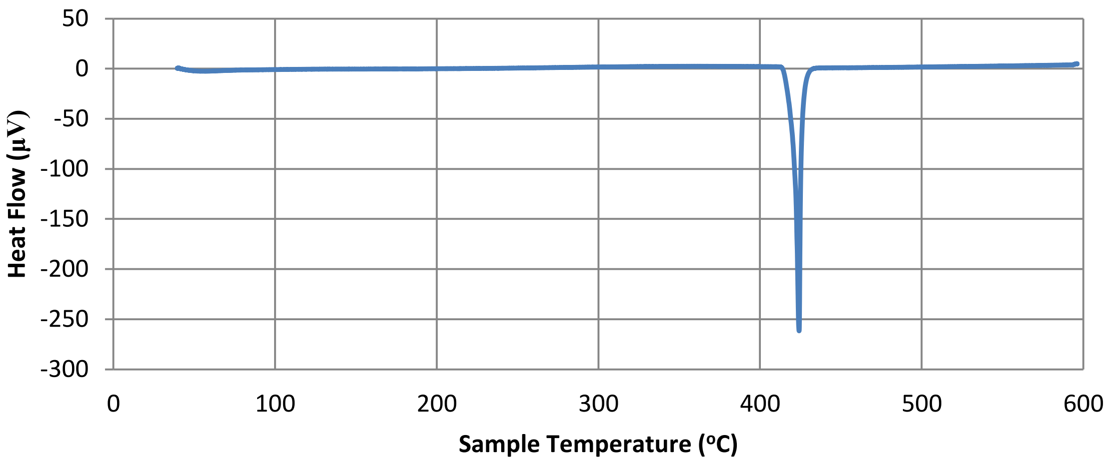

(e) Zn-1.7wt% Sb aged for 500 hours:

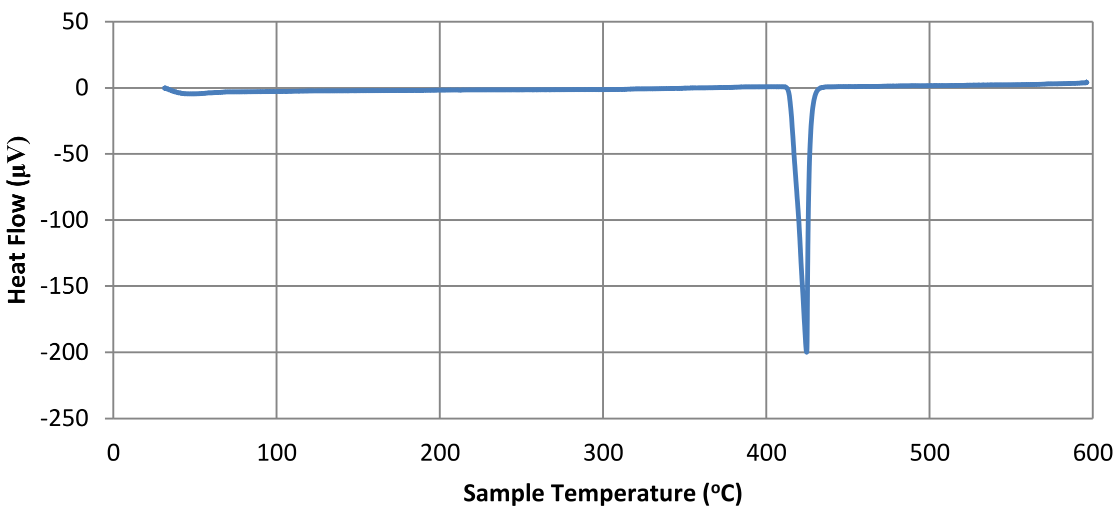

APPENDIX B

Micro Hardness for different samples of Zn-xSb alloy

Vikers Hardness test data		
Load= 1 Kg, Duration= 10 Sec		
Alloy	HV	Avg HV
Zn- 1.2wt% Sb	44.30	42.50
	40.50	
	43.70	
	42.80	
	41.20	
Zn- 1.7wt% Sb	49.80	48.38
	46.40	
	47.80	
	48.70	
	49.20	
Zn- 2.2wt% Sb	43.80	46.24
	47.20	
	46.23	
	46.40	
	47.55	
Zn- 1.7wt% Sb aged 250 hrs	57.45	55.84
	56.90	
	56.30	
	54.64	
	53.89	
Zn- 1.7wt% Sb aged 500 hrs	52.05	52.08
	55.10	
	52.56	
	49.90	
	50.78	

APPENDIX C

(a) Tensile data for Zn-xSb before ageing:

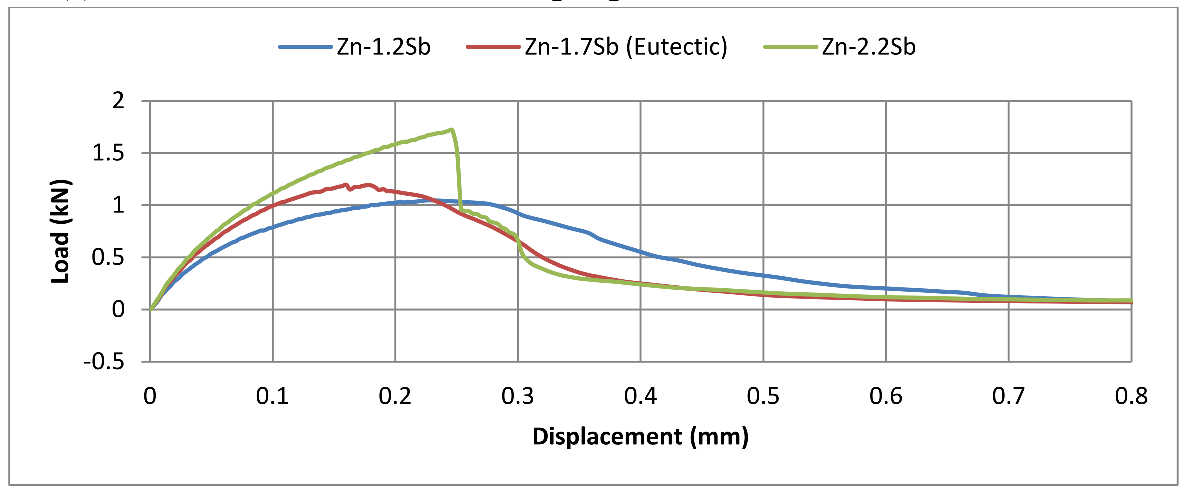

(b) Tensile data for Zn-xSb after ageing:

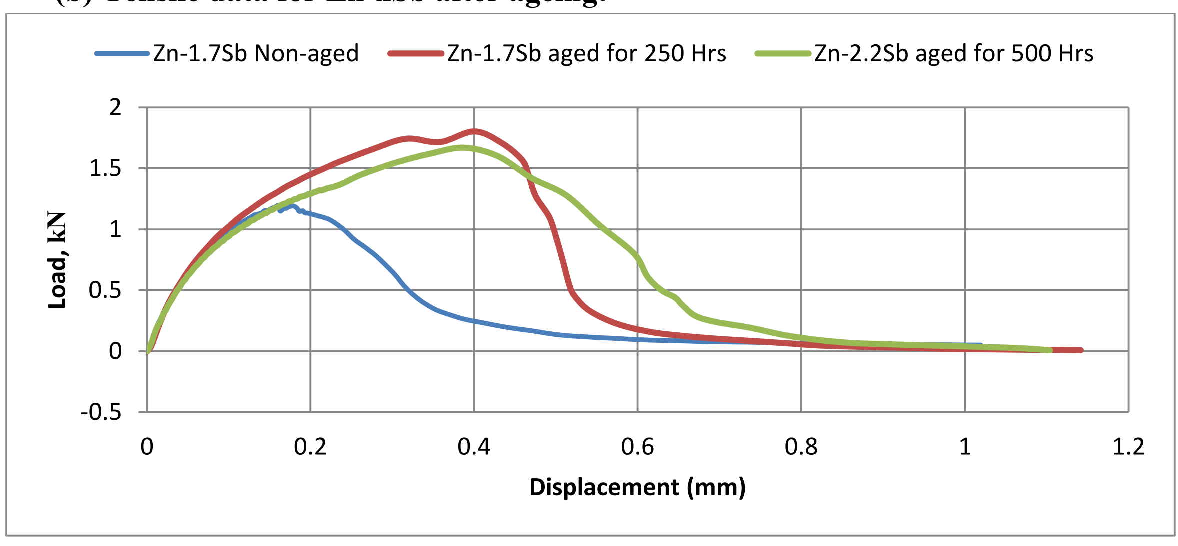

(c) Mechanical properties for Zn-xSb before and after ageing:

Alloys	Melting Behavior, (°C)	Micro hardness, (VHN)	Tensile Strength, (MPa)	Elongation, (%)
Zn-1.2wt% Sb	416.50	42.50	35	42
Zn-1.7wt% Sb	410.12	48.38	40	38
Zn-2.2wt% Sb	419.67	46.24	57	6
Eutectic aged for 250 hours	411.48	55.84	60	58
Eutectic aged for 500 hours	412.76	52.08	56	64

APPENDIX D

(a) Creep behavior of Zn-xSb before ageing:

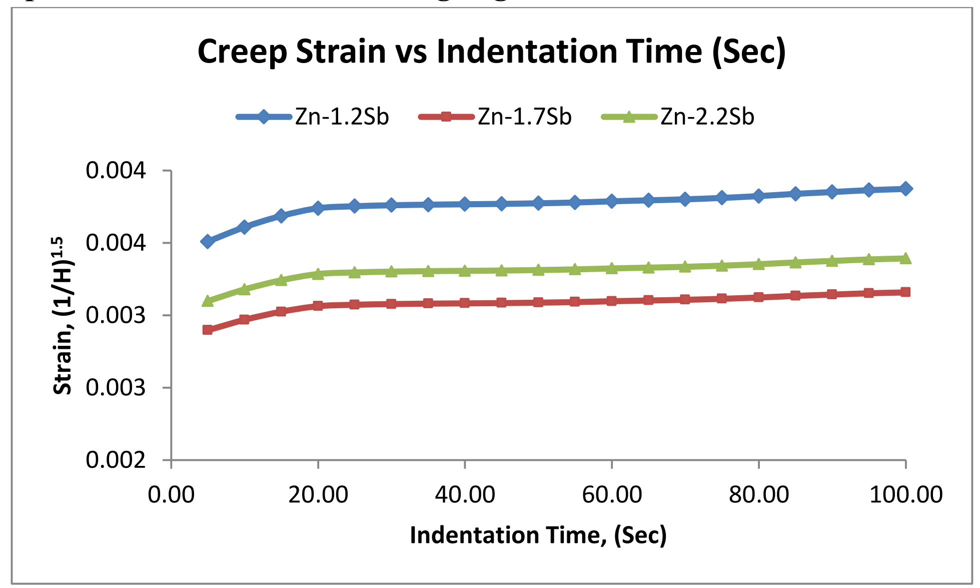

(b) Creep behavior of Zn-xSb after ageing: